Mohamed Maged Saad Abdelati Alnady

Excited State Characterization of Oligo- and Polythiophene Derivatives: Tetraphenylethene-Substituted Thiophenes, Aryl-Bithiophenes and Alternating Donor-Acceptor Indigo-Cyclopentadithiophene Copolymers

Dissertação apresentada para provas de Mestrado em Química

Orientador: Prof. Doutor João Sérgio Seixas de Melo

Co-orientador: Dr. João Pina

Setembro/2016

Universidade de Coimbra

إلى يد الله التي حمت واحتوت ودفعت للنجاح... إلى أبي الحبيب

"To the hand of God that protected, caressed and pushed

forward for success…To my beloved Dad"

Acknowledgements

In the first time of my life i feel that thanks isn't enough to show my appreciation and sincere gratitude . I came to here with a dream I wasn't fully prepared to achieve it and I would have never achieved it without the help of my group.

To Prof. Sergio Melo head of phochemistry group and my direct supervisor, thanks a lot for introducing me to your group and letting me to work in the lab with all its facilities to finish my work. Your papers were the backbone of my work and gave me a great hand to understand deeply my research point.

To Dr. João Pina my co-supervisor, Thanks for doing the best you can to help.

To the sunshine of our group that decided to rise up in different land, Dr. Catherine Castro (La Mademoiselle), seeing you working is enough to inspire anyone around you to be achieved and successful. With all the stress of work you were dedicated to, your smile and positive attitude was astonishing us. Even strongest men would feel jealous of your solid well. shine for infinity lifetime. $t_{Shining}= \infty$

To my beautiful colleagues Ana Costa and Daniela Sarmento, thanks a lot for your help with lab work, for being cooperative and flexible when it comes to scheduling the instruments. Without you I wouldn't be able to accomplish my tasks and after all thanks for your friendship.

To my God father Karim Elbadry, Ocean was pretty cold in the begining. Immigrating the comfort zone will be the most interesting thing ever.

To Everyone teached me even a word. Thank You.

Table of Contents

Figures

Tables

Schemes

Abbreviations

a. u.	Arbitrary units
HOMO	Highest occupied molecular orbital
LUMO	Lowest unoccupied molecular orbital
ε_{SS}	Singlet extinction coefficient
Λexc	Wavelength of excitation
Λem	Wavelength of emission
$_{abs}\lambda^{max}$	Wavelength of absorption maxima
$_{fluo}\lambda^{max}$	Wavelength of fluorescence emission maxima
$_{ph}\lambda^{max}$	Wavelength of Phosphorescence emission maxima
$_{T-Tn}\lambda^{max}$	Wavelength of triplet absorption maxima
ϕ_F	Fluorescence quantum yield
ϕ_{Ph}	Phosphorescence quantum yield
ϕ_{IC}	Internal conversion quantum yield
$\phi\Delta$	Singlet oxygen sensitization quantum yield
τ_F	Fluorescence lifetime
τ_{Ph}	Phosphorescence lifetime
τ_T	Triplet state lifetime
k_F	Fluorescence rate constant
k_{IC}	Internal conversion rate constant
k_{ISC}	Intersystem crossing rate constant
k_{NR}	Non-radiative processes rate constant
$\bar{M}_n$	Average molecular weight
$\bar{M}_w$	Weight average molecular weight
PD	Polydispersity

DP	Degree of polymerization
HomoPT	Tetraphenylethene polythiophene
coPT	Tetraphenylethene poly-bithiophene
P3HT	poly(3-hexylthiophene)
(T-TPE)	Tetraphenylethene thiophene
(Br-TPE)	Tetraphenylethene bromide
CPDT	Cyclopentadithiophene
C12CPDT	dodecyl-cyclopentadithiophene
Ind-CPDT	Indigo-[dodecyl-cyclopentadithiophene]

Abstract

A comprehensive investigation of the excited state properties of polythiophenes and aryl-bithiophenes has been undertaken in solution at different temperatures. The investigated polythiophenes include the tetraphenylethene-substituted -thiophene (HomoPT) and -bithiophene building blocks (coPT). In addition, and for comparison purposes, the parent poly(3-hexylthiophene), P3HT, together with the monomeric percursor tetraphenylethene-thiophene and the bromide-substituted tetraphenylethene chromophore (Br-TPE) have also been investigated. The aryl-bithiophenes consist in a common core of a benzene-bithiophene unit substituted with five different side groups; again and for comparison purposes the results of the corresponding oligothiophene terthiophene ($\alpha 3$) was used as a model compound. This includes the determination of fluorescence quantum yields, fluorescence lifetimes both in solution and in thin films at room temperature and singlet oxygen yields yields. From the obtained data, the overall set of rate constants for all the deactivation processes fluorescence, intersystem crossing, and internal conversion, were obtained; from the data, it was found that both intersystem crossing and internal conversion are important in the decay of the lowest singlet excited state of the polythiophenes and arylthiophenes in solution. An aggregation induced emission (AIE) study was also performed for both the polythiophenes and aryl-bithiophenes; in the case of the these did not display AIE in constrast with the aryl-bithiophenes where AIE is found to be present.

A complementary comprehensive investigation of the excited state characteristics of an alternating donor-acceptor Indigo-[dodecyl-cyclopentadithiophene] copolymer together with the oligomeric counterpart has been undertaken aiming to rationalize its photophysical properties. The energy transfer processes between the cyclopentadithiophene (donor) moiety and indigo (acceptor) unit and/or the occurrence of fast conformational relaxation processes in the excited state of these systems was investigated. From the overall photophysical and spectroscopic data it was seen for the oligomeric model compound and indigo-[dodecyl-cyclopentaditiophene] a high degree of electronic interaction/delocalization between the indigo and dodecyl-cyclopentaditiophene units both in the singlet and triplet excited states.

Chapter 1

Spectroscopic and Photophysical Characterization of Polythiophenes and oligomers

1.1 Introduction

Fluorescent materials have drawn considerable attention due to their wide applications in organic light emitting diodes (OLEDs), chemo- and bio-sensors, bio-imaging, etc. Most traditional luminogens, however, suffer from the notorious aggregation-caused quenching (ACQ) problem. They are highly emissive in dilute solutions while being weakly fluorescent or even non-emissive in concentrated solutions or aggregated solids. Such a thorny ACQ problem has greatly restricted their practical applications because they are normally used in aggregated or condensed solid states. It is thus essential to develop high efficiency solid emitters. To attain efficient solid- state emission, several physical and chemical approaches have to be attained. Among these methods, the construction of AIE (Aggregation Induced Emission) active compounds enjoys its unique advantage: while the other approaches try to prevent the natural aggregation process, it encourages aggregation. As opposed to ACQ dyes, AIE fluorogens are practically non-luminescent in solutions but highly emissive in aggregates, thus perfectly resolve the ACQ problem.[1]

Thanks to their high solid-state efficiencies, AIE molecules have found a variety of applications in optoelectronic devices and as bioprobes. In addition, their twisting conformations easily undergo conformation planarization under external pressure or shear stress, which would result in a remarkable emission change, thus making them highly promising as mechanochromic luminogens. The switching and tuning of solid-state emission of these smart materials is of great importance to the fundamental

research and such potential applications as sensors, memory chips, optical information storage media, display devices and security inks.[2]

Oligo-and polythiophenes are among the best investigated and most frequently used conjugated materials in particular as active componentes in organic electronic devices and molecular electronics [3]. Oligo-polythiophenes solubility could further be efficiently modulated by varying the alkyl side-groups, and good solubility was considered as a key factor for a low-cost technology. In general, appropriate long and branched alkyl groups often give rise to a close molecular packing due to the better van der Waals intermolecular interactions, arising from the nature of self-organization, which is a useful tool and approach to enhance carrier transport. The air instability of the organic field effective transistors (OFET) devices is another problem that hinders the practical applications of most organic materials. Oligo-polythiophenes containing conjugated polymers suffer from oxidative instability. Nevertheless, the introduction of fused thiophene rings to lower the energy levels of highest occupied molecular orbitals (HOMOs) could alleviate this problem. In general, air-stable p-channel organic transistors can be realized when the HOMO energy level of the material is lower than -5.0 eV.[1] Oligo- and polythiophenes, no doubt, they constitute one of the most important compound classes for photo- and electroactive molecular materials. One of the main reasons for the profound interest in oligo- polythiophenes is that their physical properties are rather unaffected by substituents.[4] In other words, they may be chemically modified in order to enhance solubility, enable processability, fine tune optical and electrical properties etc. Originally, oligothiophenes were synthesized merely to serve as model compounds for analogous polythiophenes. Stepwise oligomer syntheses, although more strenuous than traditional polymer syntheses, offer regiospecificity, precise control over chain-length and thus products easier to characterize, chemically and physically. Also, oligomers are normally more soluble than polymers, which is a key factor for the implementation of these compounds in devices. Not long after the first oligothiophenes were synthesized and evaluated, however, it became evident that they were just as, or in some cases, even more effective than polythiophenes in semiconductor applications. Most likely, this can be attributed to the fact that oligothiophenes can be synthesized and worked up to a high degree of purity (including regioisomercontrol), in contrast to polythiophenes. The term "conjugation

2

length" was invented to describe at which oligomer length (number of linked thiophene-units) the properties of a specific oligothiophene resemble those of the corresponding polythiohene. However, not all agree on this number and this rule of thumb has recently been questioned. By definition polymers are a group of organic compounds designed by repeating small blocks called monomers. Number, arrangement and type of bonds between these units affecting the complexity of polymer ; so that the study of the behavior of conjugated polymeric systems is obviously a highly complex matter , both for solids and solutions. One of the best approaches to study these complex systems is to investigate the behavior of oligomers and extrapolate the results to the polymers. As polymers are of high molecular weights comparing to other organic compounds the thing that causes challenges concerning to their solubility in solvents. the hard question is which model should be applied to interpret the spectroscopic and photophysical behavior of conjugated polymer systems given that the excitation state can't be predictable whether it is delocalized alongside the whole backbone or localized within a relatively small conjugations length. It is better to consider the second model as it is clear that the use of the properties of the corresponding oligomers can provide fundamental information needed to characterize the polymer.

1.2   Result and discussion

The structures and acronyms of the investigated compounds are depicted in Scheme 1-1. The main focus of the study will reside in the polythiophenes comprising the tetraphenylethene-substituted -thiophene (HomoPT) and -bithiophene building blocks (coPT). In addition, for comparison purposes the study of the parent poly(3-hexylthiophene), P3HT (displaying a similar degree of polymerization,DP) together with the monomeric percursor tetraphenylethene-thiophene and the bromide-substituted tetraphenylethene chromophore (Br-TPE) was performed. The average molecular weigths ($\bar{M}_n$), weight average molecular weight ($\bar{M}_w$) and polydispersities (PD) of the polymers under study are presented in Table 1.1. On the basis of the $\bar{M}_w$ data the degree of polymerization (DP) could be obtained and varies between 110 and 154 (Table 1.1).
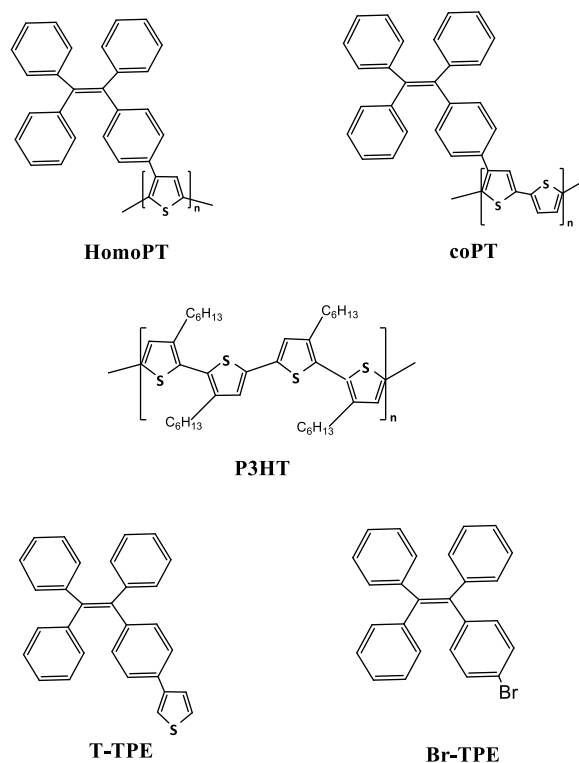
Scheme 1.1 Structures and acronyms of the compounds investigated in this chapter. Polythiophenes: Poly(3-hexylthiophene-2,5-diyl), P3HT, coPT and HomoPT polymers together with the monomeric oligothiophene model compound T-TPE and Br-TPE.

Table 1.1 Physical characteristics of the investigated polythiophenes: mean ($\bar{M}_n$) and weight average molecular weights / ($\bar{M}_w$) and polydispersity (PD); also shown is the degree of polymerization (DP) as calculated from $\bar{M}_w$.

Compound	$\bar{M}_n$ (g mol^{-1})	$\bar{M}_w$ (g mol^{-1})	PD	DP
P3HT	14000	18500	1.32	110
HomoPT	14500	57800	3.96	140
coPT	14500	76600	5.28	154

Observation of table 1.1 shows that the degree of PD of both HomoPT and coPT is high and also that the polimerization degree (DP) in these is ~50% higher that in the P3HT considered.

1.3   Spectroscopic properties

1.3.1 Singlet state in solution and solid state (thin films)

Figure 1.1 presents the absorption and fluorescence emission spectra of the investigated polythiophenes in toluene solution at T= 293 K. The spectroscopic data for P3HT shows the characteristic unstructured absorption band (in the 340–540 nm spectral range with maximum at 450 nm) and the vibronically structured fluorescence emission band also characteristic of these polythiophene derivatives.[5] Similar behaviour was observed for the lowest energy absorption band and emission spectra of the poly(tetraphenylethene-thiophenes) derivatives, thus showing that different potential energy curves (and consequently geometries) are present in the ground and first singlet excited states (see Figure 1.1).[5] This behaviour was previously reported for poly[3-(2,5-dioctylphenyl)thiophene] in toluene solution and it was attributed to the torsional relaxation of the excited conjugated segments leading to a dynamic Stokes shift.[6] It was proposed that in the ground state the chains are torsionally disordered (due to the shallow torsional potential with a nonplanar equilibrium position) and after vertical excitation the steep profile of the potential energy surface in the excited state initiates torsional relaxation into a more planar conformations (with a quinoidal-type character). Moreover, the spectroscopic properties found for P3HT closely resembles the absorption and fluorescence emission spectra found for heptathiophene ($\lambda_{máx}^{Abs}$ = 441 nm and $\lambda_{máx}^{Fluo}$ = 522 and 560 nm,[3] thus showing that the main conjugation segment for this polymers should correspond to this oligomer, that is, roughly of seven (thiophene) units in P3HT. Indeed, for the oligothiophenes counterparts it has been argued, on the basis of theoretical and experimental absorption spectra, that the segment length for intra-chain excitation correspond to ~6 monomers, while on the basis of the emission spectrum of thiophene oligomers and the measured emission spectra of P3HT, the fully relaxed emissive segment length is, in P3HT, is >7 monomers.[3,5,7]

5

Noteworthy and contrary to what was found for P3HT, is the appearrance of an additional absorption band at higher energies (325 nm) for HomoPT and coPT polymers, see Table 1.2 and Figure 1.1. Comparison with the absorption spectra of the oligomeric model compound T-TPE and Br-TPE presented in Figure 1.2, shows that, this additional spectroscopic feature is characteristic of the tetraphenylethene chromophoric unit.

In addition, when comparison is made between the lowest energy absorption band of the P3HT and the poly(tetraphenylethene-thiophenes) derivatives a red-shift of 5 nm was observed for HomoPT while a more significant 63 nm was observed for the coPT polymer (Table 1.2 and Figure 1.1). In the emission spectra no significant changes were found in the fluorescence wavelength maxima for the HomoPT when compared to the P3HT polymer (although a decrease in the vibronic structure was observed). For coPT instead, in agreement to what was observed in the absorption spectra a significant 25 nm red-shift was observed. Within experimental error the spectroscopic properties for P3HT and HomoPT can be considered identical, thus, showing that similar effective conjugation lengths (π-delocalization degree) are found in these derivatives.

Table 1.2 Spectroscopic (absorption and fluorescence emission maxima) and photophysical data (including fluorescence, ϕ_F, internal conversion, ϕ_{IC}, and singlet oxygen sensitization quantum yields, ϕ_Δ, and fluorescence lifetimes, τ_F) obtained for the investigated polythiophenes in toluene solution and in the solid state (thin films). The underlined values are the wavelength maxima.

Compound	λ^{abs}(nm) 293 K (toluene)	λ^{fluo} (nm) 293 K (toluene)	λ^{abs}(nm) 293 K (film)	λ^{fluo} (nm) 293 K (film)	ϕ_F 293 K (sol)	ϕ_F 293 K (film)	τ_F (ps) 293 K	ϕ_{IC} [a] 293 K	ϕ_Δ 293 K
P3HT	451	577	555	725	0.19	0.037	524	0.54	0.27
homoPT	325, 455	575	445	595	0.13	0.078	528	0.82	0.05
coPT	325, 513	600	513	620	0.22	0.041	715	0.68	0.10

[a] obtained using the equation $\phi_{IC}=1-\phi_F-\phi_T$ and assuming that $\phi_\Delta=\phi_T$
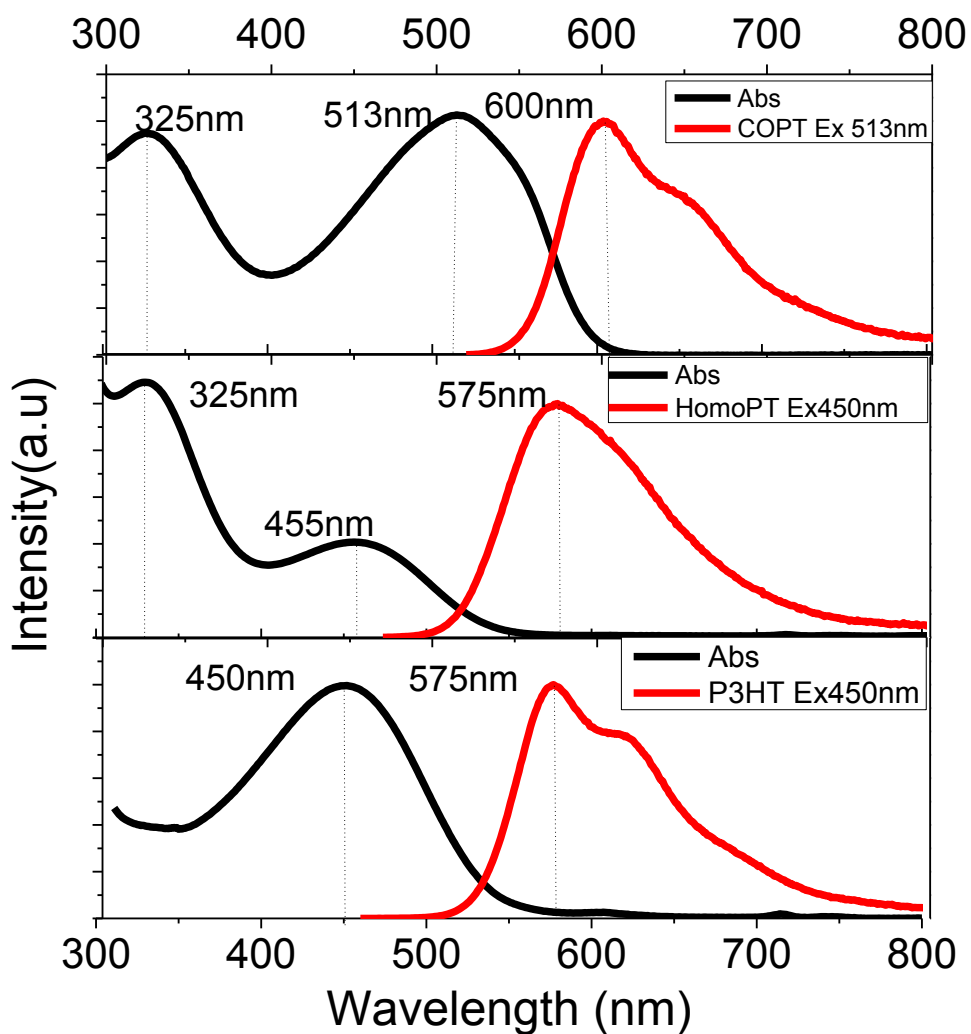
Figure 1.1 Normalized absorption and emission fluorescence spectra for the investigated polythiophenes in toluene solution at 293 K.

Figure 1.2 presents the absorption and fluorescence emission spectra of the model (oligomeric) compounds T-TPE and Br-TPE in ethanol solution at room temperature. The absorption spectrum of T-TPE and Br-TPE show the characteristic absorption band of TPE species with maximum at 320 nm for T-TPE and 310 nm for Br-TPE.[1]

In both cases the fluorescence emission spectra obtained in very diluted solutions of the compounds and collected with excitation at 330 nm presents a vibronically resolved emission band at shorter wavelengths together with an additional unstructured broad emission at lower energies likely attributed to an aggregate emission (Figure 1.2), as elsewhere described.[8] Noteworthy is to verify that the fluorescence excitation spectra when collected in the aggregate emission band matches the absorption band of the investigated compounds (Figure 1.2). Further investigation on the effect of concentration and solvent matrix on formation of aggregation induced emission properties will be investigated in section *1.3.4* of this thesis. It is also interesting to observe that substitution of a bromine atom (Br-TPE) by a thiophene group (T-TPE) does not change the spectral signature (shape and maxima) of the emission spectra but apparently leads to a 10 nm red-shift from Br-TPE to T-TPE. This seems to indicate that in the excited state the spectral characteristics are basically given by the tetraphenylethylene unit, whereas in the ground state some level of p-conjugation exists involving the TPE and thiophene units.
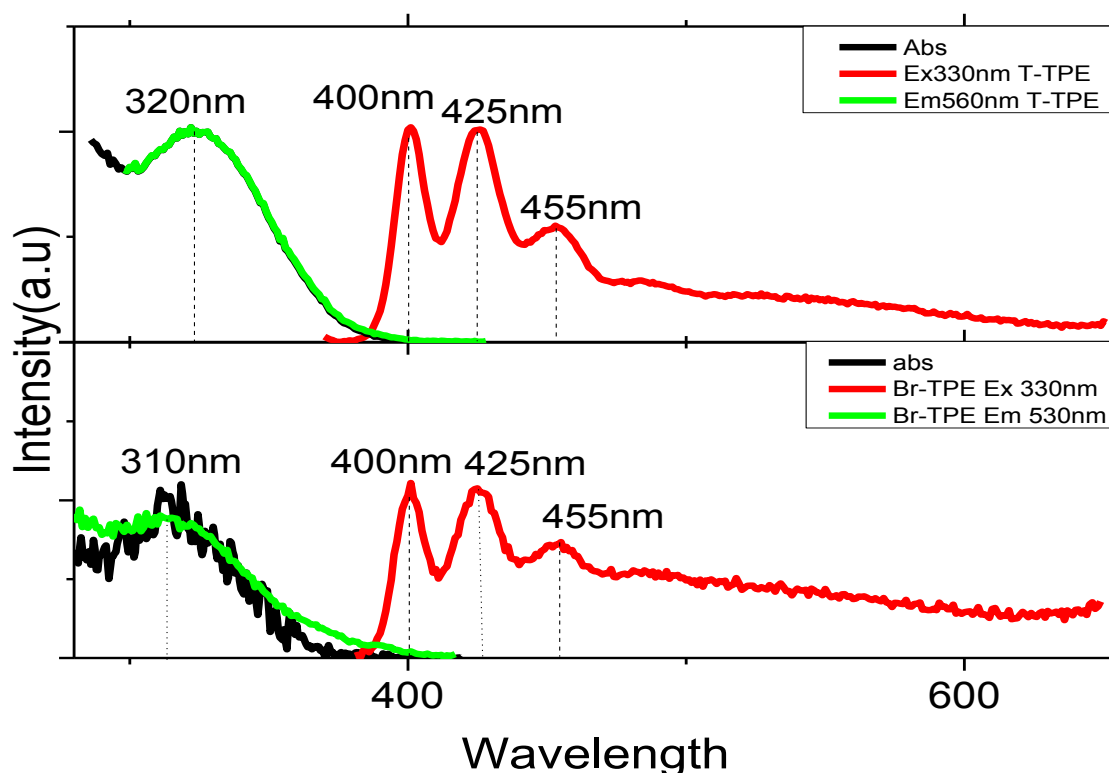
Figure 1.2 Normalized absorption spectra together with the emission and excitation fluorescence spectra for T-TPE (4.75E-6 M) and Br-TPE (1.12E-7 M) in ethanol solution at 293 K.

Figure 1.3 shows the absorption and emission spectra of P3HT both in toluene solution and in thin film at room temperature. Significant differences between the solution and solid state (thin film) excited state characteristics have been reported for many polythiophenes including P3HT, where the absorption in films becomes significantly red-shifted and more structured showing clearer peaks and shoulders.[9] In addition, upon going from solution to the solid state there is, in general a significat decrease in the fluorescence quantum yield values (see Table 1.1).[5] The large differences between the absorption and/or emission spectra obtained in solution and in thin films have been explained as a result of significant interactions between thiophene chains in solid films (aggregates formation), which extend the ground state conjugation across several chains providing a 2-D character to the electron-cloud delocalisation. [5,10] Observation of figure 1.3 shows two significant features: i) the red-shift of both the absorption and emission spectra in the solid (thin films) and (ii) the fact that in thin films the

9

absorption spectra becomes structured. This indicates that an ordered aggregate is being formed for P3HT in the solid state. As will be show in the next section with the HomoPT and CoPT polymers an almost insignificant difference between the solution and solid state behaviour is observed.

1.3.2 Aggregation induced emission (AIE)

Similar effects have been reported for aggregation of the polymer chains in mixtures of good and poor solvent.[11,12] According recent studies, the addition of bulky substituent groups to the polymer backbone[13,14] or using a regiorandom instead of regioregular arrangement of side chains on the polymer backbone[15,16], effectively increases the separation distance between polymer chains and leads to photophysical properties closer to that seen in solution.
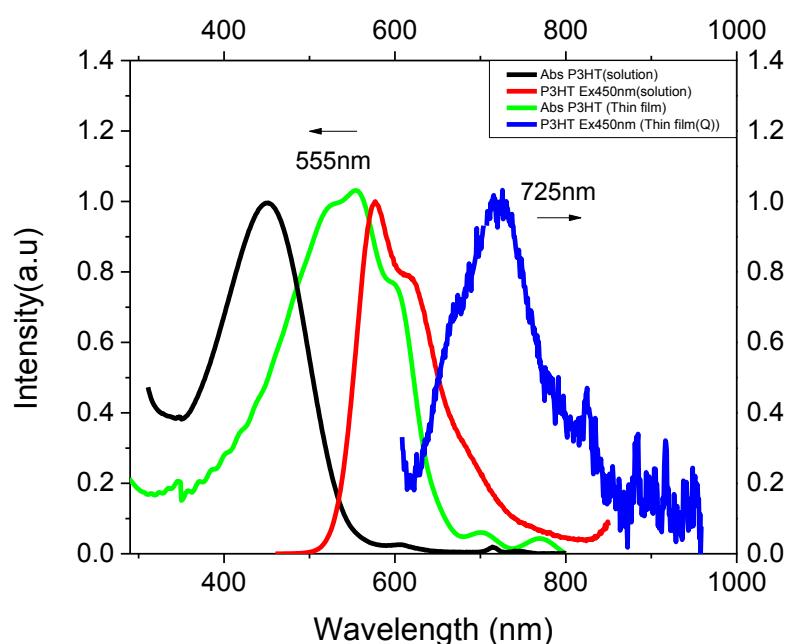
Figure 1.3 Normalized Absorption and Emission fluorescence spectra both in toluene solution and thin films for P3HT at 293K.

Figure 1.4 shows the absorption and emission spectra of HomoPT thin film alongside the absorption and emission spectra obtained in toluene solution for comparison. The thin film absorption spectra resembles the one obtained in toluene solution with slight red-shift by ~5 nm at maximum (330nm) and blue shift in the absorption band by ~10 nm at maximum (445nm). The emission spectra in thin films was found to be red-shifted by ~20 nm at maximum (595nm) when compared to the solution behaviour.

Figure 1.5 presents the absorption and emission spectra of coPT thin film together with the absorption and emission spectra obtained in toluene solution. The absorption spectra resembles that one obtained in toluene solution, whilst the emission spectra red-shifted by ~20nm at maximum (620nm).

What is relevant to stress it that in comparison with P3HT, the the HomoPT and coPT display, on going from solution to thin films, smaller red-shifts both in the absorption and emission spectra. The spectral resemblance found for these derivatives between solution and thin films and the decrease in the fluorescence quantum yields indicate that aggregation happens but in less organized structures leading to less shifted spectra.
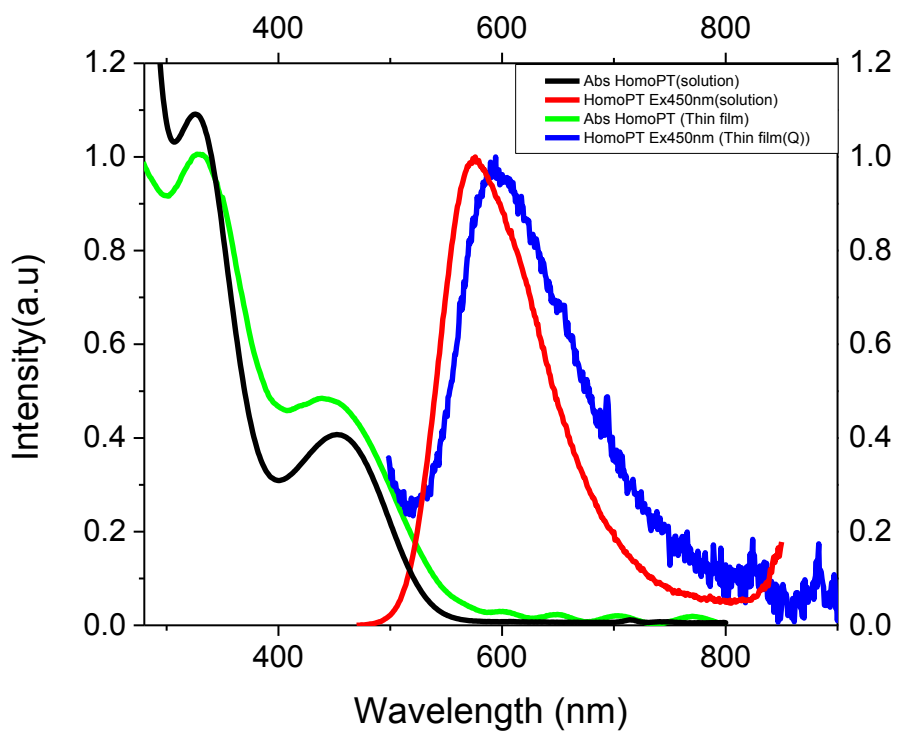
Fig. 1.4 Normalized Absorption and fluorescence emission for HomoPT both in Toluene and thin film at 293 K.
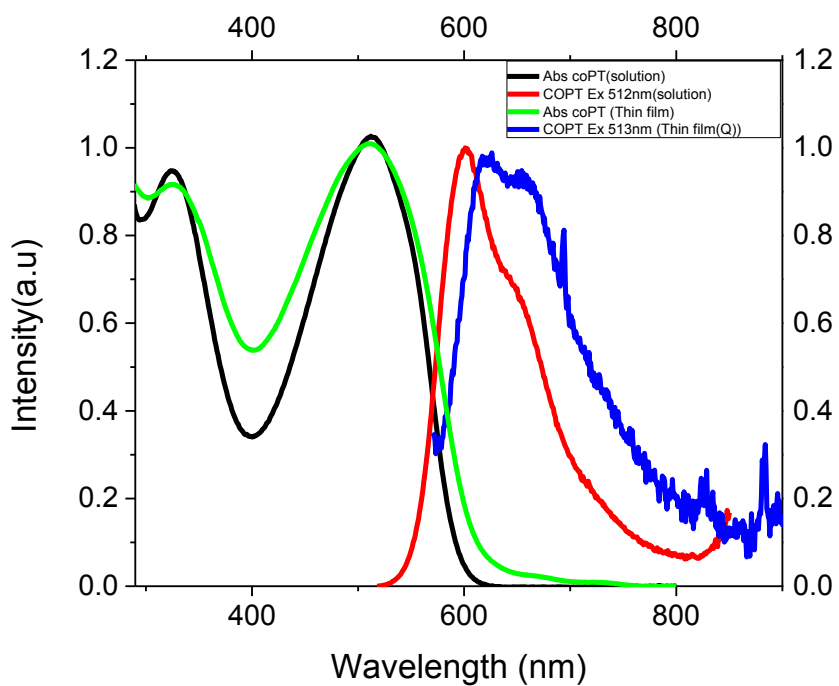
Fig. 1.5 Normalized Absorption and fluorescence emission for CoPT both in Toluene and thin film at 293 K

12

1.3.3 Time resolved fluorescence

The fluorescence decays for the investigated polythiophenes were collected in toluene solution as a function of the emission wavelength and at different temperatures. In general, for each polymer sample, the fluorescence decay times do not show any significant change when collected across the fluorescence spectra and can be considered to be independent of the emission wavelength over the whole range studied. However, the same is not valid for the pre-exponential factors, which are found to vary with the emission wavelength. This behaviour calls for a global (simultaneous) analysis of the fluorescence decays.

In general, the decays were best fitted with a tri-exponential decay law with decay time values in the 13-65 ps, 82-309 ps and 524-715 ps range (see Table 1.3 and Figure 1.6). For all the polymers the pre-exponential factors associated with the slower decay time (τ_1) increases on going from the onset to the tail of the emission band and is assigned to the relaxed and more stable (lower energy) conformation of the polymers. An opposite behaviour was found for the fast decay components where, respectively, a decrease and appearance of negative pre-exponential values were seen, on going to lower energies in the emission band. This seems to indicate that the more stable conformation of the polymers is been formed in the excited state at the expenses of two competitive processes (possibly solvent/conformational relaxation/and non-radiative intramolecular energy transfer from higher energy to lower energy chain segments).[17]

However since the energy transfer process has associated two decay components[9] .the presence (or absence) of this process can only be established from temperature dependence experiments. In the case of the conformational relaxation process, a dependence with the solvent's viscosity is to be observed.

Table 1.3 Fluorescence decays times (τ_j) and pre-exponential factors (a_{ij}) for the investigated polymers in toluene solution at 293 K. Also presented are the chi-squared values (χ^2) for a better judgment of the quality of the fits.[a]

Compound	λ_{em} (nm)	τ_3 (ps)	τ_2 (ps)	τ_1 (ps)	a_{i3}	a_{i2}	a_{i1}	χ^2
P3HT	530	13	82	524	0.75	0.15	0.1	1.12
	570				-0.203	0.103	0.897	1.06
	680				-0.838	-0.103	1	1.13
homoPT	540	65	233	528	0.471	0.473	0.057	1.16
	575				0.023	0.702	0.275	1.08
	640				-0.182	0.609	0.391	1.15
coPT	580	43	309	715	0.216	0.447	0.337	1.12
	610				0.076	0.419	0.505	1.11
	670				-0.019	0.389	0.611	1.16

[a] The data presented were obtained by global (simultaneous at the three emission wavelengths) analysis of the decays.
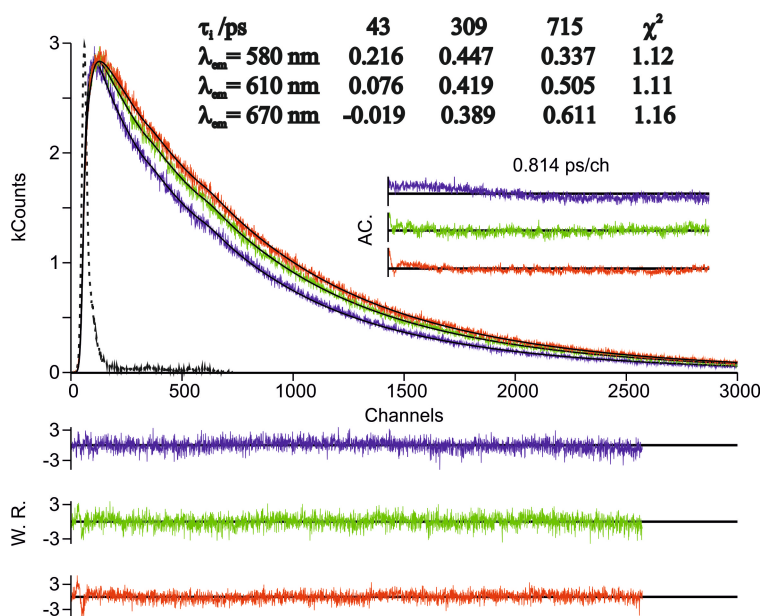
Figure 1.6 Room-temperature fluorescence decays for coPT in toluene solution. For a better judgment of the quality of the fit, weighted residuals (W.R.), autocorrelation function (A.C.) and χ^2 values are also presented. The dashed line in the decay is the instrumental response function.

1.3.3 Photophysical properties

The obtained photophysical parameters (quantum yields, lifetimes and rate constants) in solution and in solid state (thin films) are presented in Table 1.2 and 1.4. In solution the fluorescence quantum yields (ϕ_F) for the investigated polythiophenes were found to be in the 0.13-0.22 range (see Table 1.2). However, the obtained ϕ_F values should be considered to remain, within the experimental error, constant for these derivatives. In agreement to what was previously mentioned, in which similar conjugation segments should be adopted in P3HT and the tetraphenylethene-substituted polythiophenes, the constancy in the ϕ_F values also suggests that similar properties should be found in the singlet excited state of these derivatives in solution. For P3HT the value found for the room temperature fluorescence quantum yield is in good agreement to the values previously found for a regioregular polymer, RR-P3HT, with M_w= 60 kDa in toluene (work in progress) ϕ_F= 0.20, and ϕ_F = 0.33 for Mw = 55 kDa.[18]

Although triplet state formation has been reported for P3HT derivatives [9] with our current nanosecond transient absorption setup no triplet absorption signal was observed for the investigated polythiophenes. However, singlet oxygen was detected by its characteristic phosphorescence at ~1270 nm, following triplet energy transfer sensitized by these polythiophenes.

The singlet oxygen quantum yields (ϕ_D) obtained for the investigated compounds are in the 0.05–0.27 range, Table 1.2. Considering that, in general, the singlet oxygen quantum yields cannot be higher than the quantum yield of triplet formation ($\phi_D \leq \phi_T$), and that efficient singlet oxygen sensitization is observed for thiophene derivatives ($S_D = \phi_D / \phi_T$ ~1) these values can be seen as good estimate for the ϕ_T values. Thus, from the overall set of photophysical parameters including quantum yields and rate constants presented in Table 1.2 and 1.4 it can be seen that, in general, the radiationless deactivation channels ($\Phi_{IC} + \Phi_T$) are the main excited state deactivation pathways. Moreover it can also be seen that the internal conversion is the main deactivation pathways of the first excited state of these polythiophenes. This is in contrast with the behaviour found for

the oligothiophenes, where triplet state formation dominates the deactivation of these compounds.[3]

For the poly(tetraphenylethene-thiophenes), HomoPT and CoPT, although spectral similarities were found in solution and in thin films (which could indicate that similar excited states properties are found in these mediums), upon going to the solid state there is still a decrease in the in ϕ_F values (0.13 vs. 0.037 for the HomoPT and 0.22 vs. 0.041 for the coPT, respectively), see Table 1.3. Contrary to what was previously reported for P3HT polymers[18], with the poly(tetraphenylethene-thiophenes) the presence of the bulky tetraphenylethene substituents significantly hinders aggregate formation. Nevertheless, the reduction in the ϕ_F values upon going from solution to thin films should be attributed to interchain interactions, due to a better packing of the individual polymer chains in the solid state, enhancing the excited state internal conversion deactivation channel. For P3HT the absorption and emission spectral features in thin films was previously associated to the presence of aggregates/dimers and the contribution of the internal conversion deactivation channel to explain the decrease in ϕ_F on going to the solid state was ruled out. [18] Instead an alternative explanation was given, which considered the occurrence of ultrafast interchain exciton dissociation with eventual contribution of singlet-singlet annihilation (when using higher incident photon flux density excitation sources) to explain the fluorescence quenching in films. [18]

Table 1.4 Rate constants for radiative and radiationless processes obtained for the investigated polythiophenes in toluene solution.

Compound	k_F (ns^{-1})	k_{IC} (ns^{-1})	k_{ISC} (ns^{-1})	k_{NR} (ns^{-1})
P3HT	0.363	1.03	0.745	1.55
homoPT	0.246	1.55	0.211	1.65
coPT	0.308	0.951	0.325	1.09

1.3.5 Aggregation induced emission studies for T-TPE and Br-TPE

The effect of the concentration on the absorption and emission spectta was investigated for T-TPE and Br-TPE.

The absorption and emission spectra for both T-TPE and Br-TPE were monitored in different concentrations in methylcyclohexane (MCH) solution at room temperature (see Table 1.5 and Figures 1.7 and 1.8). With the increase in concentration the emission spectra, initially consisting of a single vibronically resolved band with maxima at ~400 nm, starts to present an additional broad band (with maxima at ~550 nm) that at higher concentrations becomes the only emission band which has been attributed to the characteristic aggregate emission previously reported for TPE derivatives.[19]
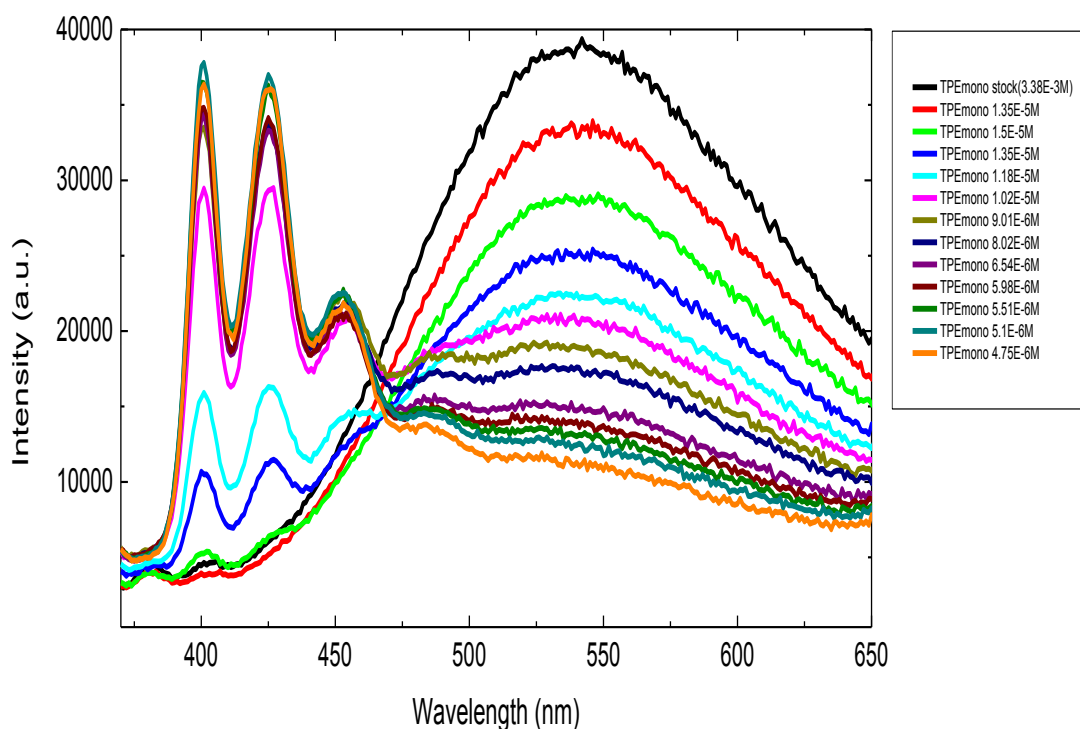
Figure 1.7 Fluorescence Emission spectra (λ_{ex}=330 nm) as a function of concentration for T-TPE in MCH solution at 293K.

Table 1.5 Spectroscopic (absorption and fluorescence emission maxima) together with the fluorescence quantum yields for T-TPE and Br-TPE obtained in ethanol solution ((4.75E-6 M) and (1.12E-7 M) respectively) and in the solid state (thin films). The underlined values are the wavelength maxima.

Compound	λ^{abs}(nm) 293 K (sol)	λ^{fluo} (nm) 293 K (sol)	λ^{abs}(nm) 293 K (film)	λ^{fluo} (nm) 293 K (film)	ϕ_F 293 K (sol)	ϕ_F 293 K (film)
T-TPE	<u>320</u>	<u>388,555</u>	<u>325</u>	<u>557</u>	0.011	0.47
Br-TPE	<u>310</u>	<u>430,473</u>	<u>315</u>	<u>475</u>	0.006	0.18

Comparing the results obtained for T-TPE and Br-TPE it can be seen that in the latter case the aggregate emission is less intense than T-TPE at higher concentrations. The aggregation induced emission (AIE) phenomenon is mainly ascribed to the restriction of intramolecular rotations (RIR).[19] Since Tetraphenylethene is more bulky than the bromide atom. It has a stronger impact on restricting the intramolecular rotations at high concentrations (aggregation solution) and films.
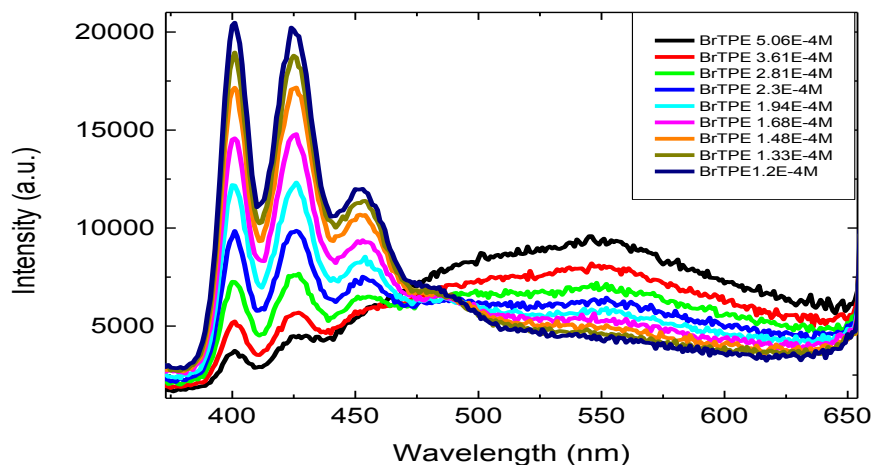
Figure 1.8 Fluorescence Emission spectra (λ_{ex}=330 nm) as a function of concentration for Br-TPE in MCH solution at 293K

Figure 1.9 shows the absorption and emission spectra of T-TPE thin film together with the absorption and emission spectra obtained in ethanol solution (1.18E-5 M) for comparison. The Absorption spectra resembles the one obtained in ethanol solution with a slight red-shift (by ~5 nm) at maximum (325 nm). The emission spectra not only is red-shifted by ~15 nm but also the vibronic structure disappeared and replaced by a broad band with maximum at 555 nm, attributed to aggregates. Similar behaviour was previously observed in TPE films where it was seen that in films the torsion of molecules decreases and the only contribution for fluorescence emission is due to aggregation induced emission. [20]

Figure 1.9 Normalized Absorption and Emission fluorescence spectra both in Ethanol solution and thin films for T-TPE at 293K.

Figure 1.10 shows the absorption and emission spectra of Br-TPE thin film alongside with the absorption and emission spectra obtained in (diluted) ethanol solution. Absorption spectra resembles that one obtained in ethanol with a slight red-shift (~ 5nm) with a maximum at 315 nm, whilst the emission spectra is red-shifted by ~50 nm with a maximum at 555 nm. Similar behaviour to what was observed for T-TPE film, was found in the emission spectra of Br-TPE film, with the induced aggregation emission prevailing in the spectra. Moreover, comparing the fluorescence quantum yields in thin films for T-TPE and Br-TPE it can be seen that the ϕ_F value for T-TPE film (0.47) is approximetely twice the value obtained for Br-TPE (0.18), this follows the trend observed in solution where T-TPE has ϕ_F that is twice that of bromine derivative. This indicates that in solution and for the two compounds,the radiationless processes are much more active than in the solid state.an explanation for this behaviour can lie on the fact that aggregation precluds,in case of the T-TPE deravative, the freedom of rotation of the thiophene unit, thus decreasing the internal conversion channel(loose

20

bolt effect)[21]. However, this doesn't fully apply to the behaviour of bromine deravative, Br-TPE.

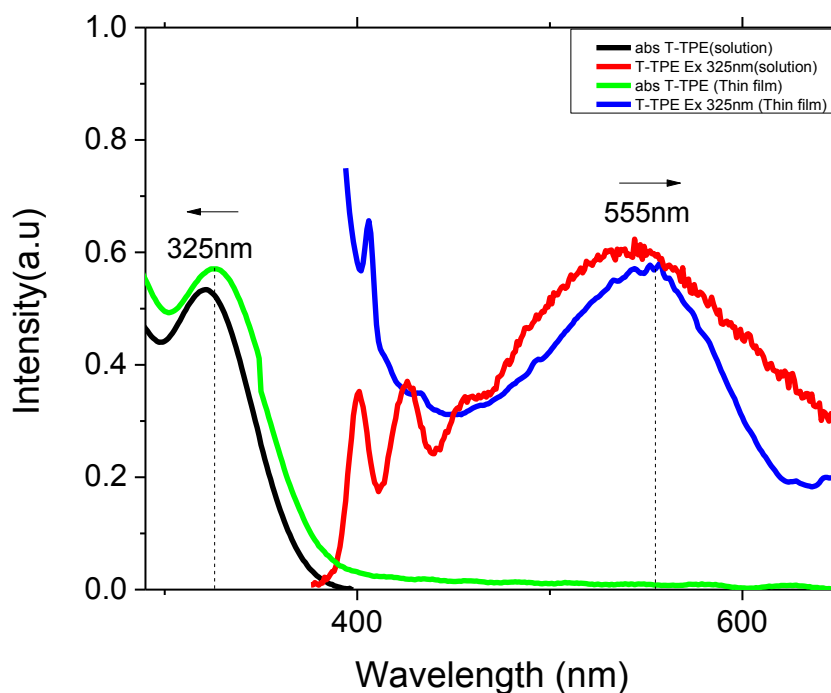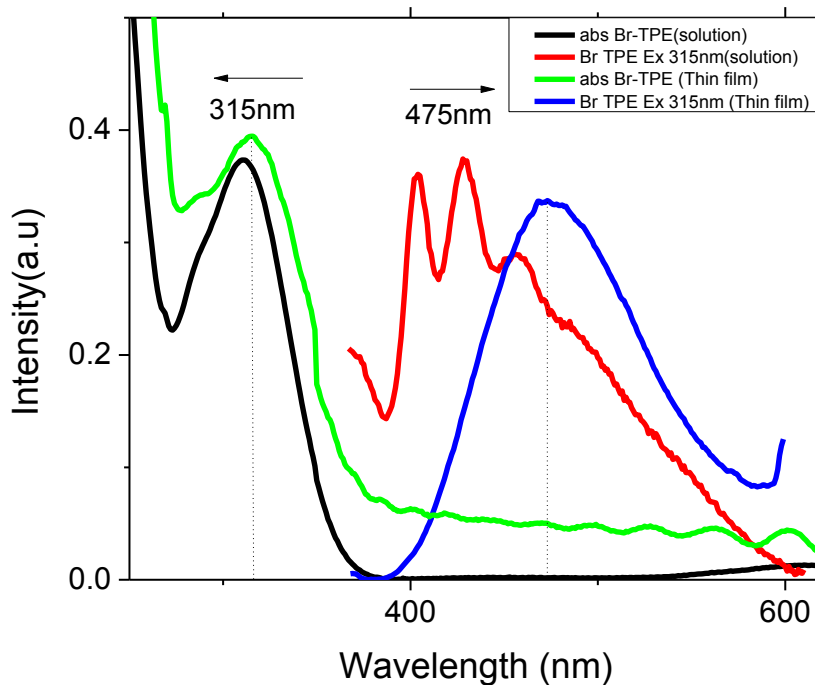**Figure 1.10** Normalized Absorption and Emission fluorescence spectra both in Ethanol solution and thin films for Br- TPE at 293K.

1.3.6 Aggregation induced emission studies for the polythiophenes

1.3.6.1. Emission

Considering that TPE is an archetype AIE luminogen, it is expected that its thiophenes-containing derivatives are also AIE-active. To check this feature, emission

behaviors of the compounds in THF and THF–water mixtures were monitored. Water was used because it is a typical co-solvent to induce aggregation of the luminogens. As can be observed in Figure 1-11, coPT shows a high fluorescence intensity with a Φ_f = 0.22 . Such a situation does not change until the water fraction (fw) reaches 10%, at which the CoPT molecules begin to aggregate and emitting with maximum at 606 nm and the Φ_f value drops down to 0.145. However, when the fw is increased to 20%, a red shift in the emission with a maximum at 613 nm is observed with a the Φ_f drasticaly decreasing to 0.041. Further increase in the fw (30% to 100%) decreases even more the fluorescence quantum yield together with slight red shift with maximum at 613nm and well defined shoulder with maximum at 665nm.

Figure 1.11 Fluorescence Emission spectra for coPT in (THF/Water) solution with different ratios of THF to water at 293K

Figure 1.12 Dependence of the Fluorescence quantum yield (in percentage) for coPT versus water fraction (fw) in THF/water mixtures at T=293K.

As shown in Figure 1.13, the HomoPT polymer displays different fluorescent behavior from the coPT in THF/water mixture solutions; indeed, a more gradual decrease (and not so steep compared to coPT, Figure 1.12) in fluorescence emission intensity and quantum yield values (see Figure 1.14) are now observed. For 0% water the HomoPT shows a Φ_f = 0.123. Such a situation does not change until the water fraction (fw) reaches 30%, at which the aggregates start to emit with maximum at 577 nm. However, when fw is increased to 50%, a red shift in the emission with a maximum at 581 nm are detected with slight decrease in intensity. Further increase in fw decreases the emission intensity with slight red shift with maximum at 581 nm. Noteworthy is that at even at fw= 100% this polymer can emit light with good intensity, Φ_F= 0.074. This behaviour makes this polymer a good candidate to be used in applications for photoimaging since water being a green solvent could be handled easily in human body without notorious effects as organic compound which most of them are reported to be carcinogenic.
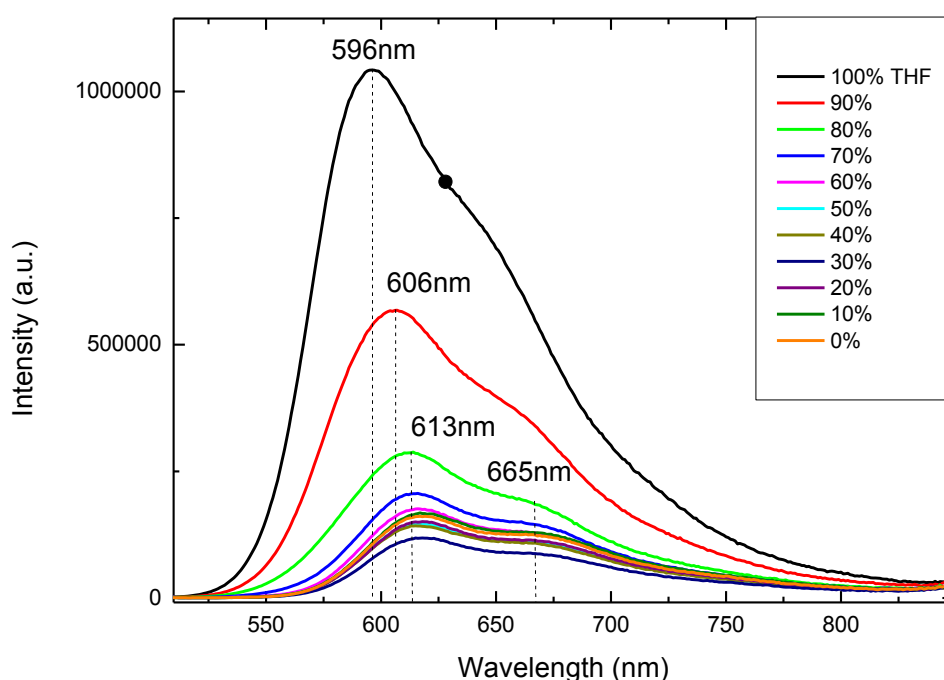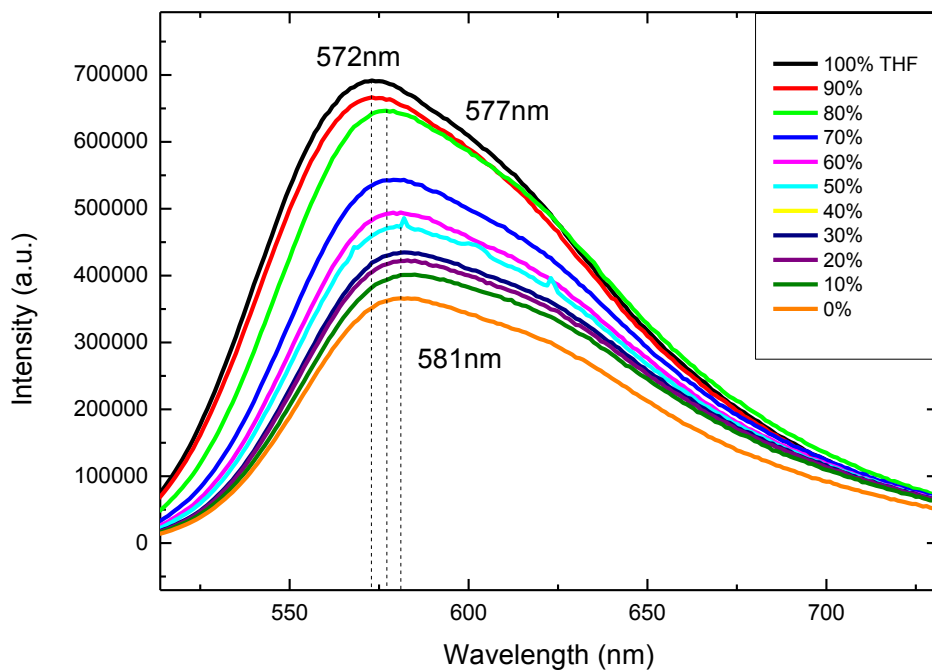
Figure 1.13 Fluorescence Emission spectra for HomoPT in (THF/Water) solution with different ratios of THF to water at 293K
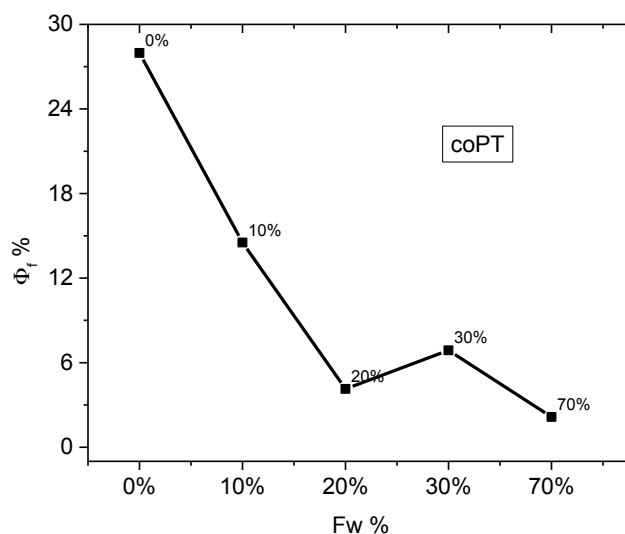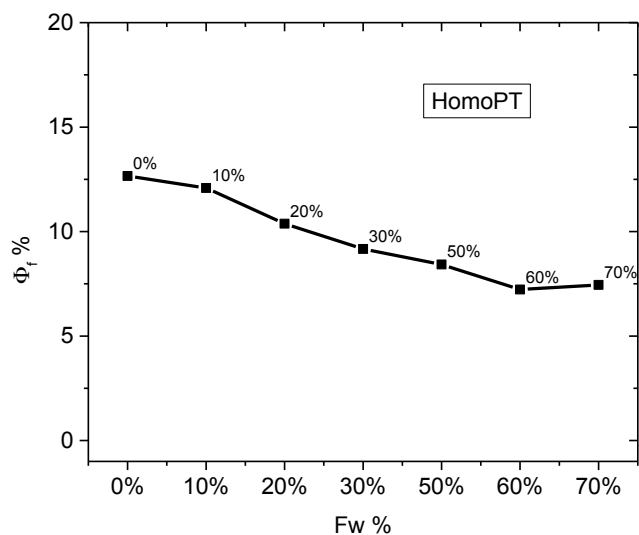

Figure 1.14 Fluorescence quantum yield percentage for HomoPT versus water fraction at 293K

The P3HT behaviour in THF/Water mixtures follows the same trend as the one observed for the previous two polymers, in which emission quenching was observed with the increase in water fraction. As shown in Figure 1.15 in pure THF the emission intensity is high with $\Phi_f = 0.278$. When the water fraction reaches 10% emission drops and $\Phi_f = 0.183$. Subsequent addition of water causes a red shift and the intensity of the first shoulder begins to decrease with a concomitant increase of the second shoulder and a decrease of the Φ_F values untill Fw reaches 50%; upon that, the Φ_f slightly increases up to 0.0197 and then drops down back. In Figure 1.15 inset this can be observed.

It can also be noticed that with increasing Fw the fluorescence emission spectra gradually red-shifts. The progressive increase in the red-shift of the fluorescence spectrum is likely due to the increase in solvent polarity[22]. From the investigation of behaviour of these polymers in THF/Water mixture we found that these we couldn't observe any induced aggregation emission , neverthless we found that even in Fw 100% they still show fluorescence emission with quite good Φ_f values ,specially HomoPT (Φ_f = 7.44%)$_{Fw=100\%}$.
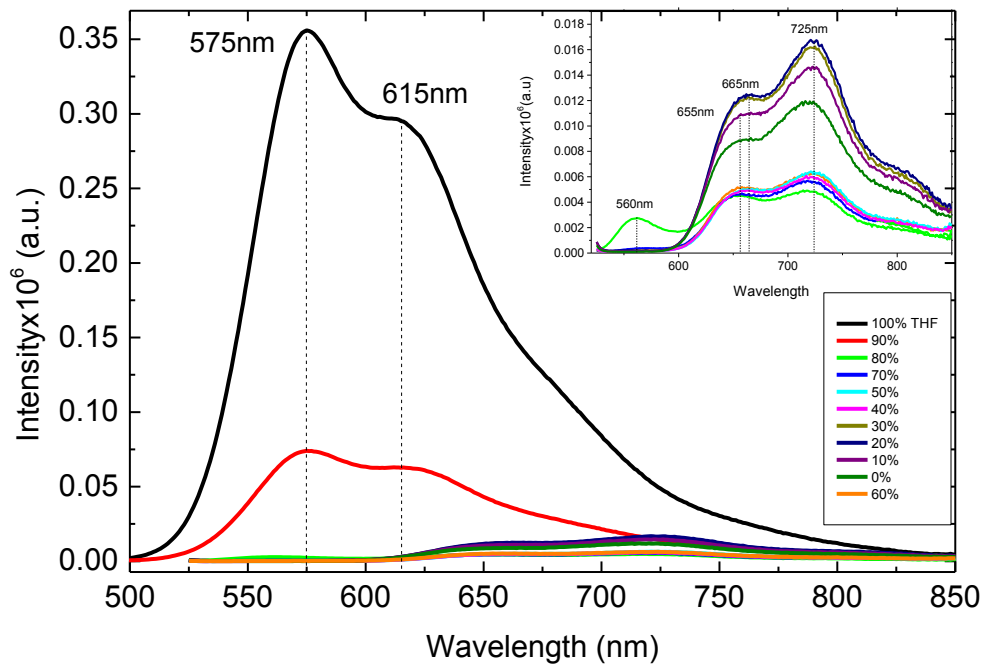
Figure 1.15 Fluorescence Emission spectra for P3HT with different ratios of THF to water at 293K, inset shows the fluorescence emission spectra for ratios (80% to 0%).
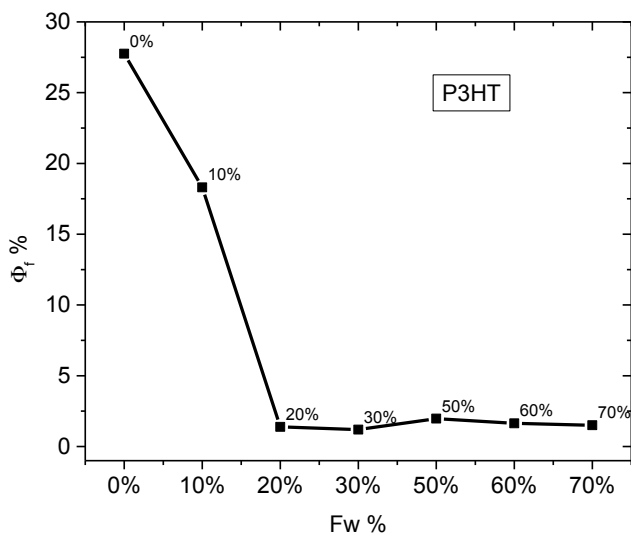
Figure 1.16 Fluorescence quantum yield percentage for P3HT versus water fraction at 293K.

1.3.6.2. Temperature Effect on the fluorescence

Figure 1.17 presents the dependence of the fluorescence emission spectra with temperature for the P3HT polymer. A clear red-shift of ~5 nm was observed when decreasing temperature together with the appearance of an additional resolved emission band at longer wavelengths for temperatures below -20 ºC. The nature of this additional band may be questioned regarding its origin: (i) either it is a consequence of a higher level of π-delocalization within the polymer or (ii) a consequence of aggregate formation. At this stage of the investigation the last hypothesis is more likely to mirror the correct nature of this observed behaviour. Indeed, this effect was observed not only in the fluorescence emission spectra (by the appearance of the additional red-shifted structured emission band, but also by the observation of a red precipitate in solution at low temperatures.
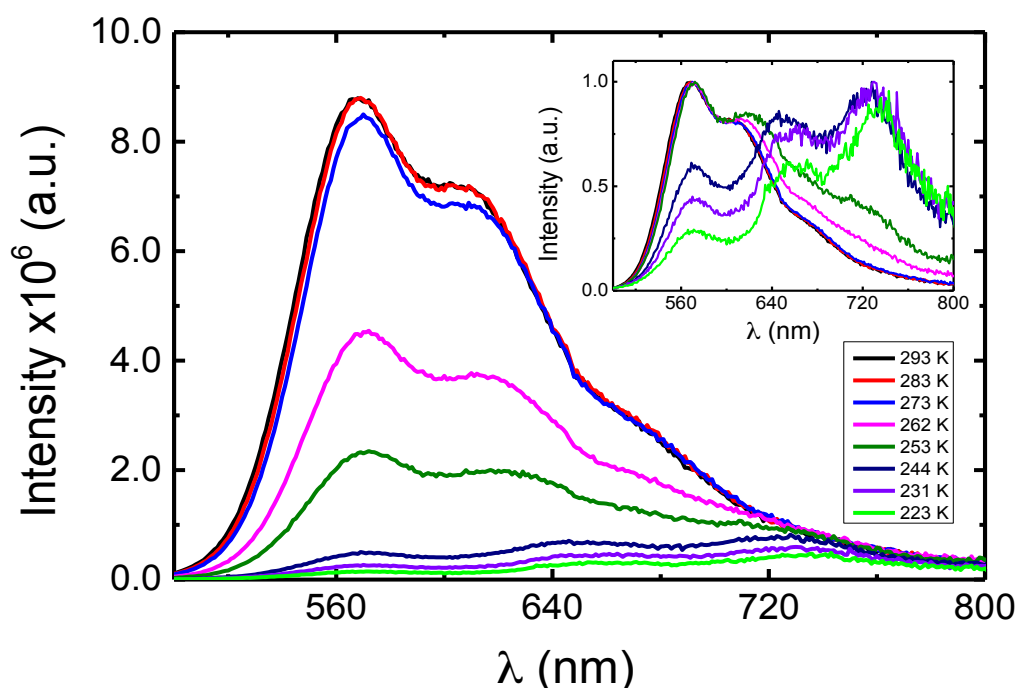
Figure 1.17 Temperature dependence of the fluorescence emission spectra of P3HT polymer in toluene solution. Shown as inset are the normalized emission spectra as a function of temperature. (λ_{ext}=445nm)

Absorption and fluorescence emission spectra of the coPT and HomoPT polymer in toluene, as a function of temperature (+20 to -60 °C) are shown in Figure (1.18a) and

Figure (1.18b) respectiveley. At 20 °C the absorption spectrum shows the broad absorption band in the 500-800 nm spectral range with maximum at 513nm (coPT) and 595 nm (HomoPT).

The fluorescence excitation spectra was also collected on the onset emission band for coPT (540nm) as shown in figure (1.19b) and also collected on the onset and tail of the emission band for HomoPT (540 and 640nm), as shown in Figure (1.19b). No additional bands appeared upon decreasing temperature that could be attributed to the formation of aggregates. This seems to indicate that in the case of the coPT and HomoPT polymer, the level of aggregation is precluded by the introduction of the TPE side group.

Varying temperature affects the fluorescence emission in a way that an increase in temperature results in a decrease in the emission intensity and concomitantly in the fluorescence quantum yield because the non-radiative processes are more efficient at higher temperatures. [22]
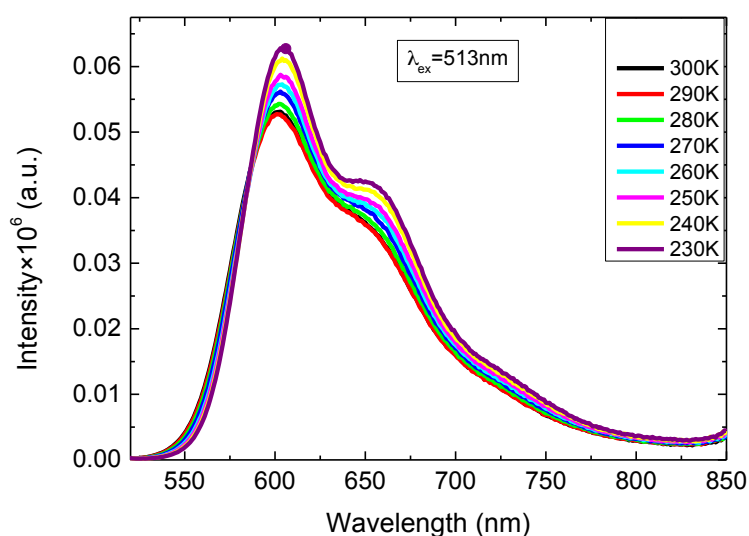
Figure 1.18a Emission fluorescence spectra obtained at (λ_{ext}=513nm)as a function of temperature for HomoPT in toluene solution.
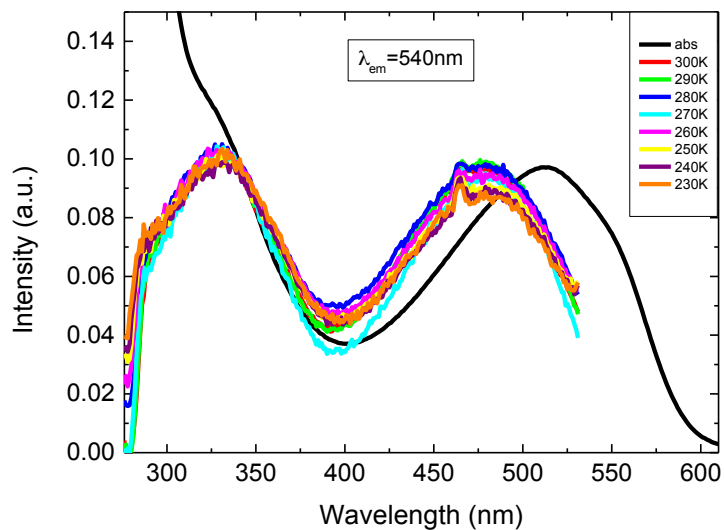
Figure 1.19a Normalized absorption and Excitation fluorescence spectra collected at 540nm as a function of temperatures for coPT in toluene solution.
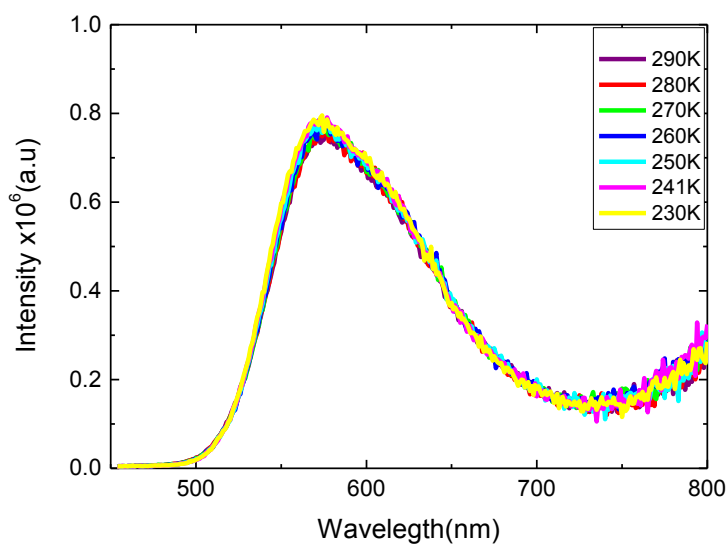
Figure 1.18b Emission fluorescence spectra obtained at (λ_{ext}=445nm)as a function of temperature for HomoPT in toluene solution.
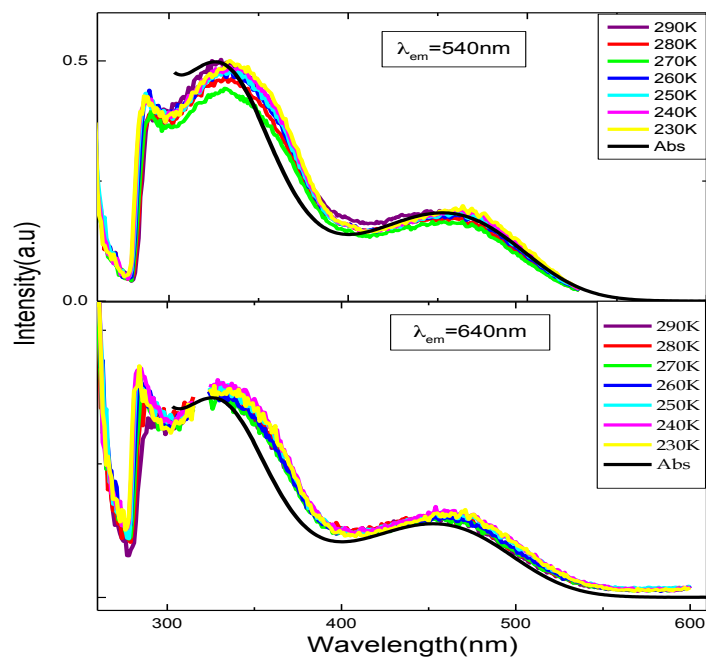
Figure 1.19b Normalized absorption and Excitation fluorescence spectra collected at 540nm (upper graph) and 640nm(lower graph) as a function of temperatures for HomoPT in toluene solution.

1.4   Conclusions

In summary, the electronica spectral and photophysical properties of a group of tetraphenylethene-substituted -thiophene (HomoPT) and -bithiophene building blocks (coPT) and for comparison the parent poly(3-hexylthiophene) have been investigatedin solution (at different temperatures) and in thin films.

From photophysical properties we noticed that the poly(tetraphenylethene-thiophenes) (HomoPT and coPT) display spectral similarities between solution and thin films; upon going to the solid state a decrease in the in ϕ_F values (0.13 vs. 0.037 for HomoPT and 0.22 vs. 0.041 for coPT, respectively) was observed which could be attributed to the presence of the bulky tetraphenylethene substituents , that significantly hinders aggregate emission in films (solid state). Similarly, with the P3HT polymer, the ϕ_F values decreased uppon going from solution to thin films ; this reduction in the ϕ_F values

should be attributed to interchain interactions, due to better packing (without aggregate formation) of the individual polymer chains in the solid state, enhancing the excited state internal conversion deactivation channel. For P3HT the absorption and emission spectral features in thin films was previously associated to the presence of aggregates/dimers and the contribution of the internal conversion deactivation channel to explain the decrease in ϕ_F on going to the solid state was ruled out.

Moreover, the photophysical properties of HomoPT and coPT can be explained by: (1) incorporation of thiophene and bithiophenes building blocks yields extra absorption bands associated with the ICT transitions, which are absent in the TPE system; (2) while TPE is AIE-active, HomoPT and coPT are typically AIE-inactive. Noteworthy is the fact that P3HT as well are AIE-inactive; even though HomoPT, coPT and P3HT do not display AIE activity, yet HomoPT displays high Φ_f values even in higher amounts (Fw=70%), which might be promising on account for applications requiring biocompatibility, which is crucial for biological applications. These unique properties of the DEA-containing TPE derivatives make them not only fundamentally interesting, but also promising for practical applications.

1.5   References

1.   Lin, Y. *et al*. Structural and Electronic Modulation of Mechanism and Application To Cell Imaging †. *J. Mater. Chem. C Mater. Opt. Electron. devices* **00,** 1–9 (2014).

2.   Ablikim, M. *et al*. Confirmation of the X(1835) and observation of the resonances X(2120) and X(2370) in J/ψ→γπ+π -η′. *Phys. Rev. Lett.* **106,** (2011).

3.   Becker, R. S., Demelo, J. S., Macanita, a L. & Elisei, F. Comprehensive evaluation of the absorption, photophysical, energy transfer, structural, and theoretical properties of alpha-oligothiophenes with one to seven rings. *J. Phys. Chem.* **100,** 18683–18695 (1996).

4.   De Melo, J. S., Burrows, H. D., Svensson, M., Andersson, M. R. & Monkman, A. P. Photophysics of thiophene based polymers in solution: The role of nonradiative decay processes. *J. Chem. Phys.* **118,** 1550–1556 (2003).

5.   Wells, N. P., Boudouris, B. W., Hillmyer, M. A. & Blank, D. A. Intramolecular exciton relaxation and migration dynamics in poly(3-hexylthiophene). *J. Phys. Chem. C* **111,** 15404–15414 (2007).

6. Westenhoff, S. *et al*. Anomalous energy transfer dynamics due to torsional relaxation in a conjugated polymer. *Phys. Rev. Lett.* **97,** (2006).

7. de Melo, J. S., Silva, L. M., Arnaut, L. G. & Becker, R. S. Singlet and triplet energies of alpha-oligothiophenes: A spectroscopic, theoretical, and photoacoustic study: Extrapolation to polythiophene. *J. Chem. Phys.* **111,** 5427–5433 (1999).

8. Liu, Y. *et al*. A tetraphenylethylene core-based 3d structure small molecular acceptor enabling efficient non-fullerene organic solar cells. *Adv. Mater.* **27,** 1015–1020 (2015).

9. Ferreira, B. Excited-State Dynamics and Self-Organization of Poly(3- hexylthiophene) (P3HT) in Solution and Thin Films. (2012).

10. Weber, C. D., Bradley, C. & Lonergan, M. C. Solution phase n-doping of C60 and PCBM using tetrabutylammonium fluoride. *J. Mater. Chem.* **2,** 303 (2014).

11. Relini, A. *et al*. Surface structure of poly(3-alkylthiophene) films studied by atomic force microscopy. *Mater. Sci. Eng. C Biomim. Supramol. Syst.* **C22,** 313–317 (2002).

12. Jain, S. & McLean, C. Proceedings of the 2003 Winter Simulation Conference S. Chick, P. J. S{á}nchez, D. Ferrin, and D. J. Morrice, eds. in *Proceedings of the 2003 Winter Simulation Conference* 1068–1076 (2003). doi:10.1109/WSC.2003.1261590

13. Perepichka, I. F., Perepichka, D. F., Meng, H. & Wudl, F. Light-emitting polythiophenes. *Advanced Materials* **17,** 2281–2305 (2005).

14. Barbarella, G., Melucci, M. & Sotgiu, G. The versatile thiophene: An overview of recent research on thiophene-based materials. *Advanced Materials* **17,** 1581–1593 (2005).

15. Rumbles, G. *et al*. Photoluminescence studies of solution thermochromism in a cyano-substituted phenylene vinylene derivative. *Synth. Met.* **111,** 501–505 (2000).

16. Jiang, X. M. *et al*. Spectroscopic studies of photoexcitations in regioregular and regiorandom polythiophene films. *Adv. Funct. Mater.* **12,** 587 (2002).

17. Banerji, N., Cowan, S., Vauthey, E. & Heeger, A. J. Ultrafast Relaxation of the Poly (3-hexylthiophene) Emission Spectrum. *J. Phys. Chem. C* **115,** 9726–9739 (2011).

18. Cook, S., Furube, A. & Katoh, R. Analysis of the excited states of regioregular polythiophene P3HT. *Energy Environ. Sci.* **1,** 294 (2008).

19. He, B. *et al*. Aggregation-enhanced emission and efficient electroluminescence of conjugated polymers containing tetraphenylethene units. *Sci. China Chem.* **56,** 1221–1227 (2013).

20. Rumbles, G. *et al*. Chromism and luminescence in regioregular poly(3-dodecylthiophene). *Synth. Met.* **76,** 47–51 (1996).

21. Turro, N. J., Ramamurthy, V. & Scaiano., J. C. *Modern Molecular Photochemistry of Organic Molecules*. *Angewandte Chemie International Edition* (2010). doi:10.1002/anie.201003826

22. Valeur, B. *Related Titles from WILEY-VCH Analytical Atomic Spectrometry with Flames and Plasmas Handbook of Analytical Techniques Single-Molecule Detection in Solution . Methods and Applications*. *Methods* **8,** (2001).

23. Dogariu, A., Vacar, D. & Heeger, A. J. Excited state spectral and dynamics studies of MEH-PPV. *Synth. Met.* **101,** 202–203 (1999).

24. Lemaur, V. *et al*. Charge Transport Properties in Discotic Liquid Crystals: A Quantum-Chemical Insight into Structure-Property Relationships. *J. Am. Chem. Soc.* **126,** 3271–3279 (2004).

25. Marder, S. R. *et al*. Large first hyperpolarizabilities in push-pull polyenes by tuning of the bond length alternation and aromaticity. *Science* **263,** 511–4 (1994).

26. Ridolfi, G. *et al*. All-thiophene donor–acceptor blends: photophysics, morphology and photoresponse. *J. Mater. Chem.* **15,** 895–901 (2005).

27. Pawlicki, M., Collins, H. A., Denning, R. G. & Anderson, H. L. Two-photon absorption and the design of two-photon dyes. *Angewandte Chemie - International Edition* **48,** 3244–3266 (2009).

28. Raposo, M. M. M. *et al*. Synthesis and characterization of dicyanovinyl-substituted thienylpyrroles as new nonlinear optical chromophores. *Org. Lett.* **8,** 3681–3684 (2006).

29. Melo, J. S. De, Pina, J., Burrows, H. D. & Brocke, S. The effect of substitution and isomeric imperfection on the photophysical behaviour of p -phenylenevinylene trimers. **388,** 236–241 (2004).

30. Genin, E. *et al*. Fluorescence and two-photon absorption of push–pull aryl(bi)thiophenes: structure–property relationships. *Photochem. Photobiol. Sci.* **11,** 1756 (2012).

31. Melo, S. De, Batista, R. M. F., Costa, S. P. G. & Raposo, M. M. M. Synthesis and Characterization of the Ground and Excited States of Tripodal-like. *Synthesis (Stuttg)*. 4964–4972 (2010).

32. McKendrick, K. G. *Principles and Applications of Photochemistry*. *Journal of Modern Optics* **36,** (1989).

Chapter 2

Photophysical properties of π-conjugated oligomers induced by different electron donor groups

2.1 Introduction

Polarized π-conjugated molecules end-capped with electron donors (D) and acceptors (A) with intra-molecular charge-transfer (ICT) represent promising organic materials for optoelectronics. Such D-π -A molecules possess several remarkable properties such as well-defined structure with tunable optoelectronic properties, distinctive color, high dipolar character, and intrinsic (hyper)polarizabilities. In this respect, thiophene proved to be one of the most polarizable π-conjugated heterocyclic unit used for the design of D-π-A molecules whilst it is used as auxiliary electron-donor type has also been reoported. [1,2]

Aryl-Bithiophenes have been applied in applications such as non-linear optics (NLO)[3] and biology[4]. In particular, the past decade has been marked by a growing interest in the design of NLO chromophores for two photon absorption (TPA) applications. These efforts have been driven by the various applications of the TPA phenomenon in different fields including material science, biology and medicine.[5]

In addition, for easier detection in biological media and tissues, red-emitting fluorophores are particularly helpful. In this context, we have been interested in investigating the potentialities of recently published push–pull oligothiophene derivatives whose second-order optical responses have been shown to be of interest.[6] Unlike previous works that gave focus on studying the characteristics of push-pull approach for aryl-bithiophenes end capped(double substituted) with electron donating and electron withdrawing groups, the goal of this study is to investigate the effect in the photophysical properties in these π-conjugated oligomers induced by substituting only one side by different electron donor groups. Another motivation will be the investigation of the AIE properties has elsewhere reported for aryl-thiophene derivatives.

2.2 Results & Discussion

The structures and acronyms of the investigated compounds are depicted in Scheme 2-1. These consist of five aryl-bithiophenes substituted with different electron donor groups.
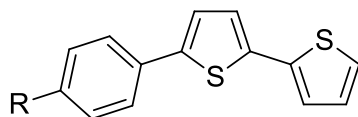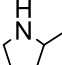
4a-e

a R= H
b R= MeO
c R= EtO
d R= NEt$_2$
e R= pyrrolidine

Scheme 2.1 Structures of the investigated aryl-bithiophenes

2.2.1 Steady state in room temperature vs low temperature

The absorption spectra of the aryl-bithiophenes in ethanol solution at room and low temperature, 77 K, (here represented by the fluorescence excitation spectra) are shown in Figure 2-1. At room temperature, the spectra are broad and structureless. In solution at 293 K, the absorption (band and wavelength maxima) red shifts upon going from hydrogen substituent to pyrolidine (H<MeO≅EtO<NEt$_2$≅Pyrrolidine). Upon decreasing the temperature, an increase in the vibronic structure and a red shift of the spectra occurs when compared to the spectra at 293 K, with changes in absorption maxima ranging from ~25 nm (**4a**) to ~20 nm (**4e**), as shown in Table 2.1. In the room (293 K) versus low temperature (77 K) spectra, the most dramatic changes are, however, observed for the compounds with weak electron-donor groups **4a, 4b** and **4c,** with a clear increment of the vibronic resolution at 77 K.

36
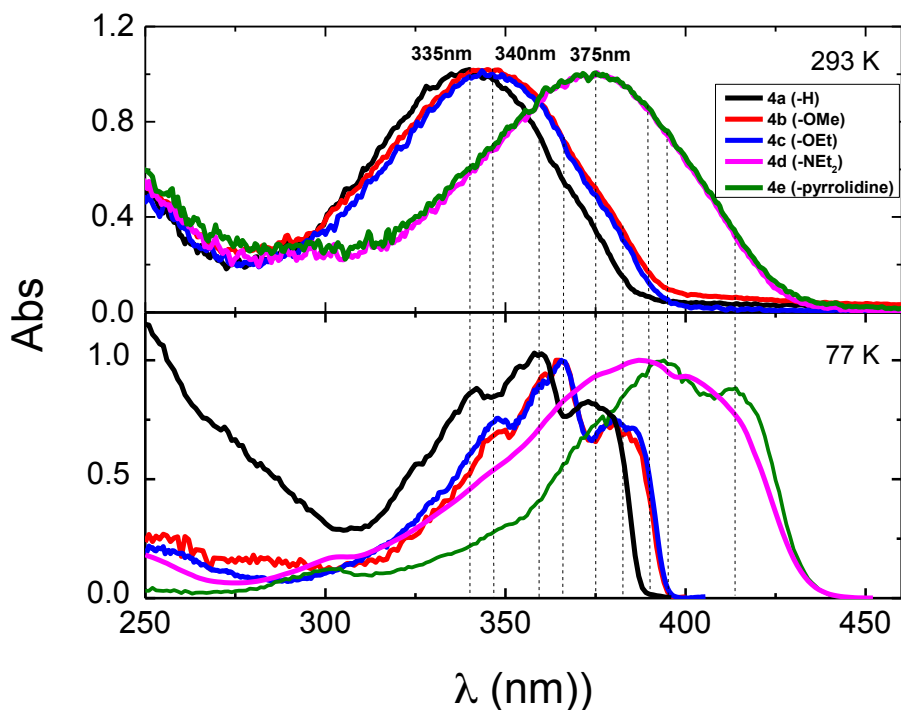
Figure 2.1 Normalized absorption spectra for the investigated aryl-thiophenes in ethanol solution at 293 K and 77 K (collected from the fluorescence excitation spectra).

In Figure 2.2 the fluorescence emission spectra in solution at 293 K and 77 K are shown. Upon going from 293 K to 77 K there is a marked increase in the vibronic structure of the spectra in agreement to what was found in the absorption spectra. However, contrary to what was seen in the absorption, in the emission a blue shift by ~40 nm for both (**4d**) and (**4e**) was observed upon going from 293 to 77 K. A similar behavior was previously found for naphthalene end-terminated oligothiophenes that was attributed to the ground state to which the more planar excited state (quinoidal-like) deactivates.[7] However, in the present case compounds 4d and 4e show not only blue shift of the emission maxima on going from 293 K to 77 K, but an increase in vibronic resolution (the emission band at 293 K is broad and devoid of vibronic resolution) and the nature of the substiuent groups -diethylamino, **4d** and pyrrolidine, **4e**- it seems that a charge transfer transition is present (likely involving the nitrogen donor and bithiophene acceptor) that likely becomes more localized at 77K which could partially explain the red-shift in the absorption and blue shift in emission. This should be further confirmed with quantum mechanical calculations.
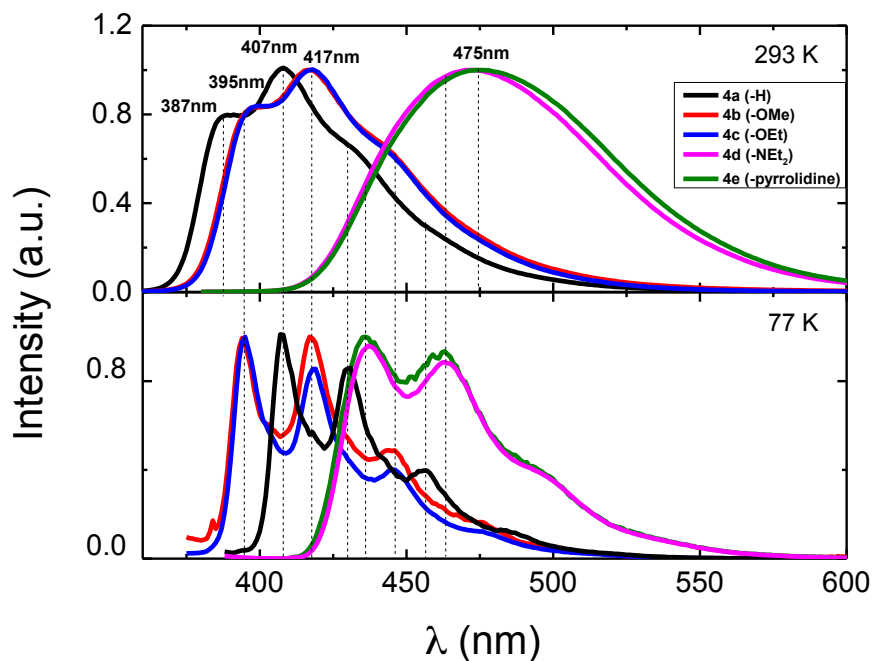
Figure 2.2 Normalized fluorescence emission spectra for the investigated aryl-thiophenes in ethanol solution at 293 K and 77 K.

Also relevant to this discussion is the observation that the spectroscopic data at 293 K for **4a**, **4b** and **4c** are similar to that found for α-terthiophene, **α3** (see Table 2-1), which shows that the benzene ring unit adds the equivalent of one thiophene unit to the π-conjugation length of the S_1 state of these compounds. Fluorescence lifetimes were measured in solution at room temperature and were all seen to be well fitted with single-exponential decay law (see Figure 2.3 and Table 2.2).
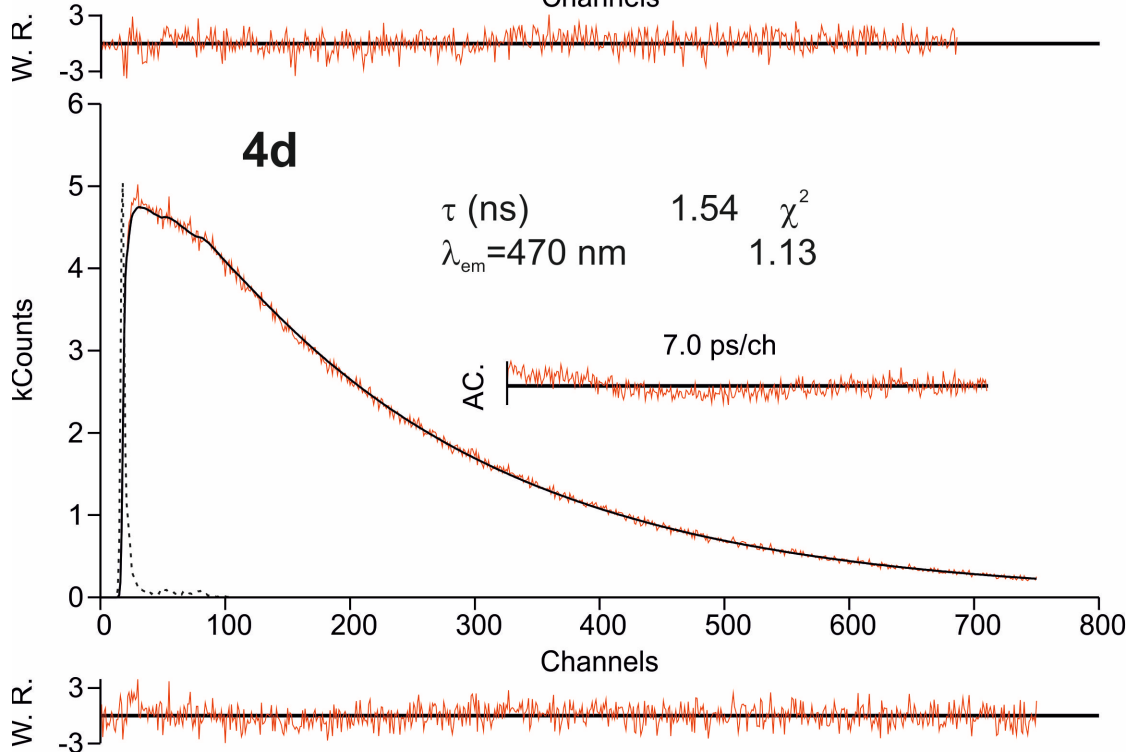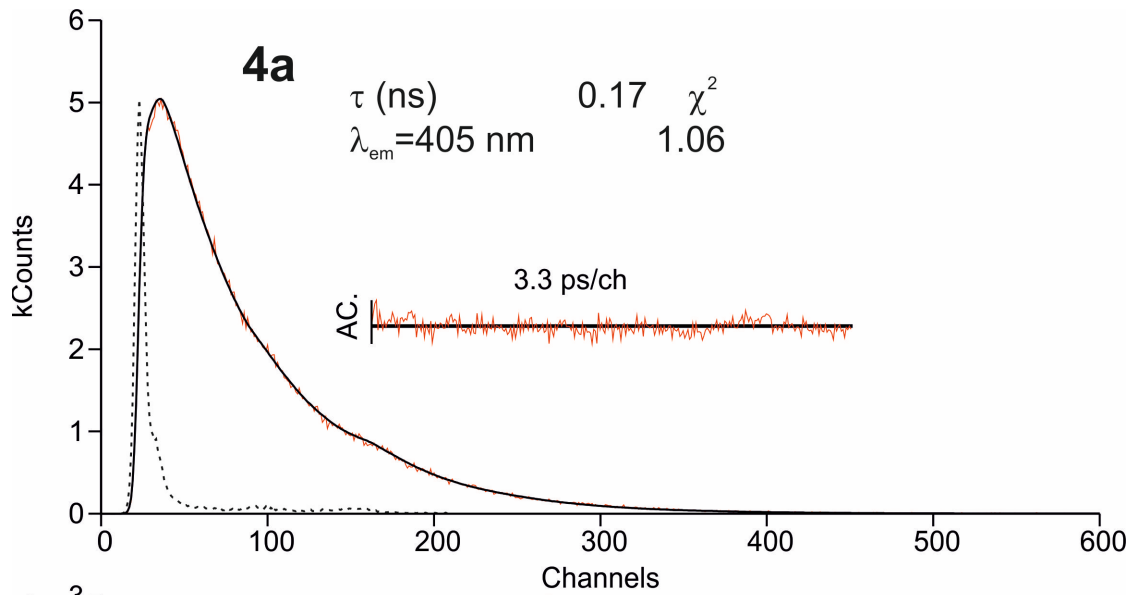
4a

τ (ns)   0.17 χ^2
λ_{em}=405 nm   1.06

AC.   3.3 ps/ch

4d

τ (ns)   1.54 χ^2
λ_{em}=470 nm   1.13

AC.   7.0 ps/ch

2.2.2 Triplet-State and Singlet Oxygen Sensitization

Upon laser flash photolysis at 355 nm of degassed solutions of the aryl-thiophenes in ethanol at 293 K, depletion of the ground-state absorption was observed at lower wavelengths together with an intense transient absorption band with maxima at longer wavelengths (Figure 2.4). The triplet-triplet absorption spectra are broad suggesting delocalization of the triplet excited state due to conjugation along the oligomers chains. From Table (2.2) and Figure (2.4) it can be observed the constancy in the T_1-T_n wavelength maxima when going from 4a to 4c. In contrast, an increase in the T_1-T_n maxima was observed with the increase of strength of donor side group in the oligomer chain (4d and 4e), see Figure 2.4 and Table 2.2.
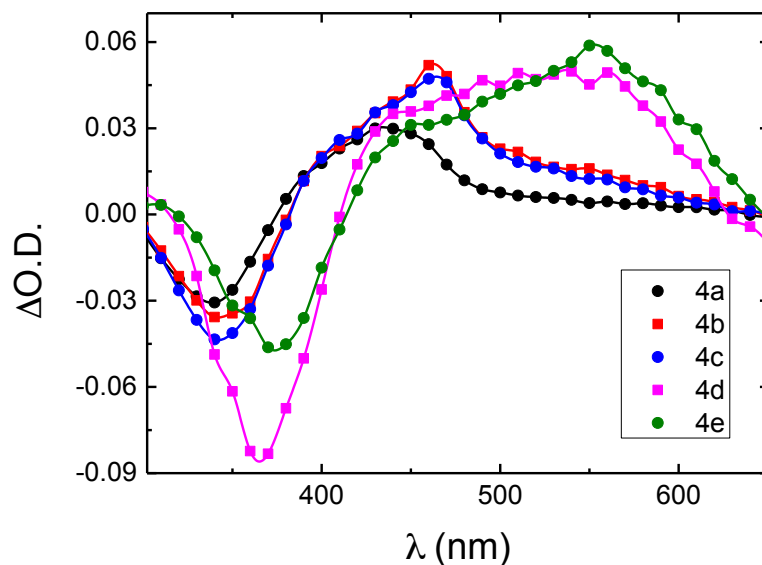
Figure 2.4 Normalized singlet-triplet difference absorption spectra for the investigated aryl-thiophenes in ethanol solution at 293 K.

Table 2.1 Spectroscopic data (absorption, fluorescence and triplet absorption maxima for the investigated compounds in ethanol solution at 293 K. Underlined values are the wavelength maxima.

Compound	$293K\lambda^{abs}$ (nm)	$77K\lambda^{abs}$ (nm)	$293K\lambda^{Fluo}$ (nm)	$77K\lambda^{Fluo}$ (nm)	$_{max}\lambda^{T1-Tn}$ (nm)	ε_{ss} (cm^{-1})
4a	335	340,<u>360</u>,375	387,<u>407</u>	<u>407</u>,430,455	435	5431
4b	340	347,<u>365</u>,380	395,<u>417</u>	395,<u>417</u>,445	460	5005
4c	340	347,<u>365</u>,380	395,<u>417</u>	395,<u>417</u>,445	460	5005
4d	375	390	475	<u>435</u>,463	550	5614
4e	375	<u>395</u>,415	475	<u>435</u>,463	550	5614
α3 [a]	352	354, <u>372</u>, 388	405, <u>426</u>	403, <u>427,</u> 455	460	4935

[a]α-Terthiophene, **α3**, data was included for comparison

The photophysical parameters obtained in solution at 293 K and 77 K are presented in Table 2.2. In agreement to what was previously observed for the unsubstituted α3, for compounds 4a-c the intersystem-crossing radiationless channel (obtained assuming $\phi_T \approx \phi_\Delta$) is the main excited state deactivation channel. However, an opposite behaviour to that found for α3 (where the internal conversion decay channel was negligible, ~0) was seen for the investigated aryl-bithiophenes (with the exception of derivative 4a). In the present case the internal conversion radiationless decay process is active with values in 0.08-0.24 range, see Table 2.2. Upon going to the aryl-bithiophenes derivatives with the higher electron–donor character strength, 4d and 4e, there is a significant increase in the ϕ_F values (by ~7 times) compared to derivatives 4a-c. For the formers the radiative channel can now strongly compete with the radiationless processes ($\phi_T + \phi_{IC}$), accounting with ~50 % for the excited state decay of these derivatives (see Table 2-2). The increase in ϕ_F with the increase in the strength of donorability of the side group in the oligomer backbone agrees with the general trend observed with the oligothiophenes and its derivatives. [8]Upon cooling from 293 K to 77 K the fluorescence quantum yield increases for all the investigated compounds, with the exception of

derivatives **4b** and **4d**. Similar effect was also reported for the unsubstituted oligothiophenes and was associated to the conformational degrees of freedom of these oligomers at 293 K, which is reduced at 77 K, thus enhancing the contribution from the radiative decay channel. [9] For **4b** and **4d** instead, the constancy observed in the ϕ_F values suggest that similar excited state structures are adopted at 293 K and 77 K for these derivatives. It is also worth noting that the fluorescence lifetimes for **4a**, **4b** and **4c** resembles those found for the corresponding oligothiophene **α3**, thus giving further support that for the investigated aryl-bithiophene derivatives the phenyl ring acts as an efficient substitute for one thiophene unit. [9]

Table 2.2 Photophysical properties including quantum yields (fluorescence, ϕ_F, internal conversion, ϕ_{IC}, and sensitized singlet oxygen formation, ϕ_Δ, lifetimes τ_F (ns) ,τ_τ (µs)) for the investigated samples in ethanol solution.

Compound	ϕ_F (293 K)	ϕ_F (77 K)	τ_F (ns) (293 K)	ϕ_{IC} [a] (293 K)	ϕ_Δ (293 K)	τ_τ (µs)
4a	0.066	0.12	0.17	0.12	0.82	53
4b	0.078	0.09	0.18	0.24	0.68	46
4c	0.071	0.17	0.17	0.01	0.92	41
4d	0.51	0.52	1.54	0.08	0.41	48
4e	0.51	0.62	1.73	0.19	0.3	4
α3	0.054	0.12	0.19	0	-	91

[a] obtained using the equation $\phi_{IC}=1-\phi_F-\phi_T$ and assuming that $\phi_\Delta=\phi_T$

[b] Terthiophene, α3, data was included for comparison[10]

2.2.3 Aggregation induced emission studies

The emission behaviour of some of the investigated compounds (4a and 4e) was insvestigated in THF and THF–water mixtures. As can be observed in Figure 2.5 and 2.6, compound 4a shows a decrease in the Φ_f values till the fraction of water reaches 50%, while the Φ_f value slightly increases from 0.052 to 0.066 . This situation continues till

fraction of water reaches 70% and the Φ_f value is 0.075 and then further addition of water leads to a decrease in the Φ_f values.

Figure 2.5 Fluorescence Emission spectra for 4a in (THF/Water) solution with different ratios of THF to water at 293K.

Figure 2.6 Fluorescence quantum yield percentage for 4a versus water fraction at 293K.

Unlike 4a, 4e (Fig. 2.7) shows aggregation induced emission behaviour (AIE), with a gradual red-shift in the emission band (with the ~50nm shift upon going from 100% THF for the 30:70 v/v THF/water mixture reflecting the aggregation phenomena) and increase in Φ_f values with the increasing of the water fraction. Aggregation is believed to be induced due to the increase in steric hinderance and rigidity of 4e as a result of the pyrrolidine side group at benzene ring. [11]
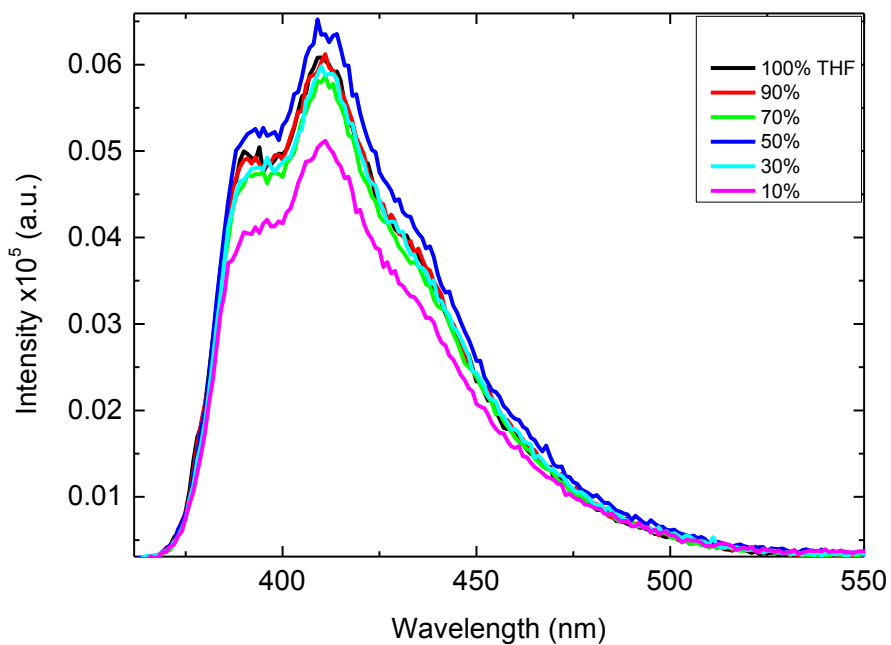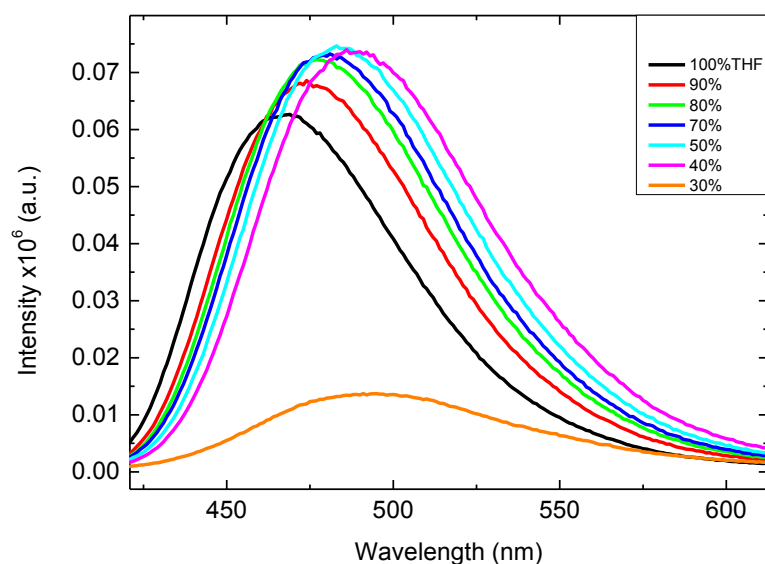

Figure 2.7 Fluorescence Emission spectra for 4e in (THF/Water) solution with different ratios of THF to water at 293K.
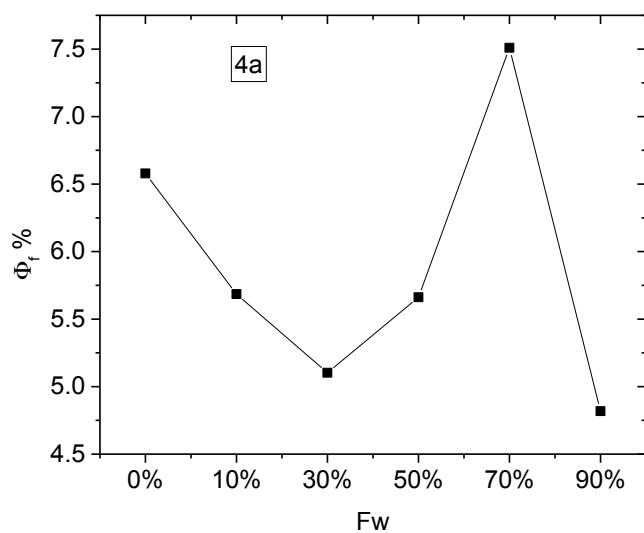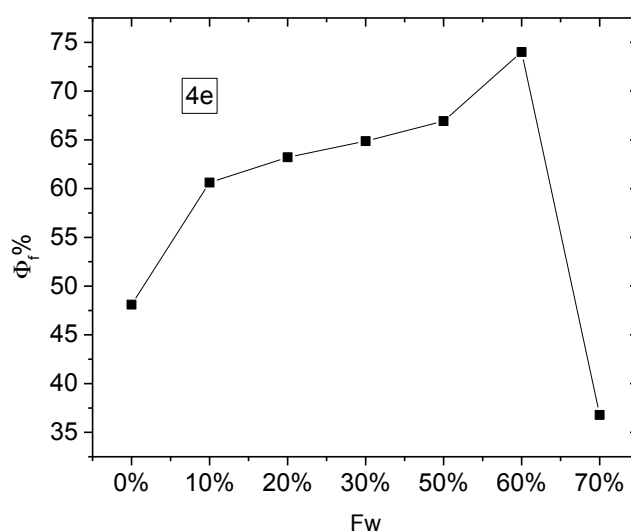

Figure 2.8 Fluorescence quantum yield percentage for 4e versus water fraction at 293K

44

2.3 Conclusions

An investigation of the photophysical properties of aryl-bithiophenes monosubstituted derivatives, these π-conjugated oligomers induced by the different electron donor groups. The electronic spectral and photophysical properties were investigated in solution and the AIE properties was also done. From the photophysical data in solution it was shown that these oligomers present significantly higher Φ_f values (1 order of magnitude) than the corresponding oligothiophenes **α3**, for compounds 4d and 4e while φ_F values for compounds 4a,4b and 4c changes slightly. the substituents diethylamine and pyrrolidine increase the conjugated system and made the benzene ring mimic the same effect of thiophene rings in higher oligothiophenes **αn's**. from the AIE studies we could see that AIE properties depend on the nature of the substituent. 4a does not display AIE properties while 4e showstrong AIE properties in high water fractions (Fw%), in (Fw =60%) (Φ_f =75%) . It was also seen that for compounds 4a-c the intersystem-crossing radiationless channel (obtained assuming $\phi_T \approx \phi_\Delta$) is the main excited state deactivation channel. However, an opposite behaviour to that found for a3 (where the internal conversion decay channel was negligible, ~0) was seen for the investigated aryl-bithiophenes (with the exception of derivative 4a). In the present case the internal conversion radiationless decay process is now active with values in 0.08-0.24 range. Upon going to the aryl-bithiophenes derivatives with the higher electron–donor character strength, 4d and 4e, there is a significant increase in the ϕ_F values (by ~7 times) compared to derivatives 4a-c. For the formers the radiative channel can now strongly compete with the radiationless processes ($\phi_T + \phi_{IC}$), accounting with ~50 % for the excited state decay of these derivatives. The increase in φ_F with the increase in the strength of donor side group in the oligomer backbone agrees with the general trend observed with the oligothiophenes and its derivatives.

The next step in this study is the characterization of these aryl-bithiophnes derivatives and oligomeric counterpart in the solid state and their thermal stability to evaluate there potential use for applications such as light-emitting devices.

2.4 References

1. Dogariu, A., Vacar, D. & Heeger, A. J. Excited state spectral and dynamics studies of MEH-PPV. *Synth. Met.* **101,** 202–203 (1999).

2. Lemaur, V. *et al.* Charge Transport Properties in Discotic Liquid Crystals: A Quantum-Chemical Insight into Structure-Property Relationships. *J. Am. Chem. Soc.* **126,** 3271–3279 (2004).

3. Marder, S. R. *et al.* Large first hyperpolarizabilities in push-pull polyenes by tuning of the bond length alternation and aromaticity. *Science* **263,** 511–4 (1994).

4. Ridolfi, G. *et al.* All-thiophene donor–acceptor blends: photophysics, morphology and photoresponse. *J. Mater. Chem.* **15,** 895–901 (2005).

5. Pawlicki, M., Collins, H. A., Denning, R. G. & Anderson, H. L. Two-photon absorption and the design of two-photon dyes. *Angewandte Chemie - International Edition* **48,** 3244–3266 (2009).

6. Raposo, M. M. M. *et al.* Synthesis and characterization of dicyanovinyl-substituted thienylpyrroles as new nonlinear optical chromophores. *Org. Lett.* **8,** 3681–3684 (2006).

7. Melo, J. S. De, Pina, J., Burrows, H. D. & Brocke, S. The effect of substitution and isomeric imperfection on the photophysical behaviour of p -phenylenevinylene trimers. **388,** 236–241 (2004).

8. Genin, E. *et al.* Fluorescence and two-photon absorption of push–pull aryl(bi)thiophenes: structure–property relationships. *Photochem. Photobiol. Sci.* **11,** 1756 (2012).

9. Becker, R. S., Demelo, J. S., Macanita, a L. & Elisei, F. Comprehensive evaluation of the absorption, photophysical, energy transfer, structural, and theoretical properties of alpha-oligothiophenes with one to seven rings. *J. Phys. Chem.* **100,** 18683–18695 (1996).

10. Melo, S. De, Batista, R. M. F., Costa, S. P. G. & Raposo, M. M. M. Synthesis and Characterization of the Ground and Excited States of Tripodal-like. *Synthesis (Stuttg).* 4964–4972 (2010).

11. McKendrick, K. G. *Principles and Applications of Photochemistry. Journal of Modern Optics* **36,** (1989).

Chapter 3

Spectroscopic and Photophysical Characterization of Alternating Donor-Acceptor Indigo-Cyclopentadithiophene Copolymers

3.1 Introduction

Indigo, with more than 5000 years of history, is one of the oldest organic dyes to be used as a blue colorant for painting and dyeing.[1] The longevity of this dye has historical reasons and has been linked to its worldwide spread distribution, with more than 700 Indigofera (natural provenance of the dye) species known, to cultural aspects (linking for example the Western and Muslim civilizations), medicinal uses (for example of its isomer indirubin[2] with several applications including leukemia treatment and also to the genesis of the German[3](and consequently European) chemical industry, recognized by the 1905 Nobel Prize in Chemistry awarded to A. von Baeyer for the first proposed synthetic indigo. The longevity of indigo is chemically related to its high stability towards light (photostability) which has been associated to the high efficiency of the radiationless internal conversion channel.[4,5] Due to the low solubility of indigo in the majority of organic solvents the idea of a polymer built of indigo has probably never been properly equated. Despite the pioneer works of G. Heller[6] in 1903 who prepared a polymeric indigo but could not realize the polymeric nature of the dye[7] the first report of a detailed characterization of a polymer of indigo is dated from 1990 with the work of Tanaka et al.[8] who prepared a polymer with an indigo unit in the main skeleton, and found that the polymer was insoluble but possessed a fraction that was attracted to a permanent magnet therefore displaying magnetic properties. More recently Voss et al.[7] prepared and characterized two similar statistical copolymers made of indigo and N-

acetylindigo units with defined structures in solution and in the solid state. With the recent recognition of the potential and importance of organic conjugated polymers for photovoltaic applications, including isoindigo based conjugated polymers[9,10] a polymer of indigo is of relevance since it would potentially generate long lived and stable charged species (whose radiative deactivation is negligible), a requisite which is mandatory for this type of applications.

Indigo has been shown to owe its high bathochromicity (shift to longer wavelengths) to the special orientation of the electron donor (NH) and acceptor (C=O) groups, see Scheme 1.[10] Depending on the nature of the substitution (electron-donating or withdrawing) the relative energy of the HOMO and LUMO will be affected through the donor and acceptor group characteristics. The donor and acceptor groups can be influenced by peripherical substitution at the indigo benzene rings. In addition to its peculiar bathochromacity, indigo is also one of the most stable dyes used technologically. The strong and surprisingly bathochromic absorption in indigoid dyes originates from the so-called indigoid H-chromophore, a cross-conjugated arrangement of electron donor and acceptor groups.[10] Thus, the low-energy visible absorption occurs due to charge transfer from the electron-rich NH groups to the electron-poor carbonyl functions. It is known that electron-rich substituent in the 6,6'-positions inductively push electron density onto the carbonyl groups, decreasing their electron-accepting character and therefore hypsochromically shifting the absorption of the indigoid H-chromophore.
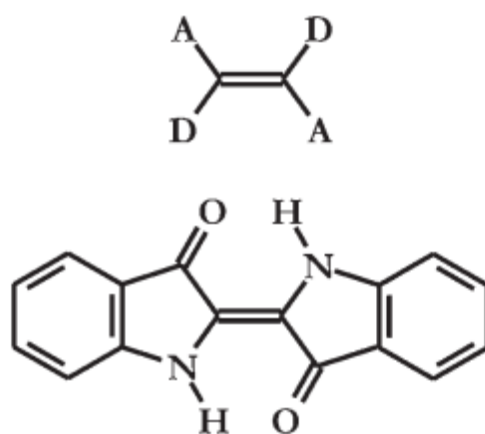
Scheme 3.1 Structure and chromic system of indigo

Indigo and its derivatives have been used as dyes and pigments for thousands of years by many of the world civilizations. In the 19th century, the high commercial value of indigo dyestuffs encouraged early organic chemists to explore synthesis routes to indigos, and indeed the economic race to develop synthetic indigos was a major impetus behind the development of modern synthetic organic chemistry.[11,12]

Recently, it was found that indigo and derivatives show considerable potential for organic electronic applications. In field-effect transistors, indigos have shown ambipolar operation with mobility in the range 0.01–1.5 $cm^2V^{-1}s^{-1}$.[13] These materials stand out in particular due to excellent operational stability in air, with minimal performance degradation even after measuring for >1 year.[13] In parallel, there have been extensive studies reported in the literature on semiconducting properties of the closely related building blocks, namely, isoindigos and diketopyrrolo-pyrroles[14,15], where these chromophores work as electron-accepting units in donor–acceptor type polymers. Indigos themselves were overlooked for such applications, as they are considered to have poor intramolecular π-conjugation.[16] Nevertheless, in crystalline thin film indigos adopt cofacial packing with sufficient transfer integral between neighboring molecules to support charge transport. Formation of highly crystalline film is driven by the interplay of (π-π) stacking and intra- and intermolecular hydrogen bonding (H-bonding).

Indigo has two other known structural isomers: Isoindigo and indirubine. copolymers derived from isoindigo can be considered as green polymers. Isoindigo has a strong electron-withdrawing ability due to the diimide functional group. Many isoindigo based D–A conjugated polymers have been reported.[refs] The results indicate that the isoindigo based D-A conjugated polymers exhibit broad absorption, well matched energy level with PCBM acceptors and high charge mobility, showing that isoindigo can be a promising acceptor unit for constructing ideal D–A conjugated polymers.[17] The solubilizing side chains attached on the backbone of the isoindigo copolymer are necessary for the ease of solar cell fabrication.[17]

Polymers containing indigo as an acceptor unit in the main chain were reported, with large side chains attached to the nitrogens of the indole moiety in order to increase solubility. These materials show promising n-type behavior with an electron mobility of ~10^{-3} $cm^2V^{-1}S^{-1}$.[18]

Conjugated polymers comprising alternating electron donor (D) much attention recently as active semiconductors for organic thin film transistors (OTFTs) and organic photovoltaics (OPVs).[19] Polymer solar cells (PSCs) as an alternative to inorganic photovoltaic devices have become the focus of intense research due to their lightweight, flexibility and ease of large-scale fabrication. A typical PSC consisting of the active layer which is usually basedon the bulk heterojunction (BHJ) concept and is fabricated from blending of the electron donor (conducting polymers) and electron acceptor (fullerene derivatives). To achieve a high efficiency BHJ solar cell, several factors in molecular structures (e.g., conjugated backbone and side chains) must be rationally taken into consideration. The donor–acceptor (D–A) strategy is widely applied to design the backbone of the conjugated polymer. By combination of the electron-donating moiety and electron-withdrawing moiety, the energy level of the resulting alternating conjugated copolymer can be fine-tuned through intramolecular charge transfer (ICT) and lead to a narrow band gap (1.2–1.8 eV) and thereby can absorb more light in the visible and infrared region. Although vast D–A low band gap polymers were developed, it is still a challenge to develop an ideal and sustainable low band gap polymer with appropriate choice of donor and acceptor units. Recently, band gap control in linear π-conjugated systems has been intensively studied because the band gap is the key factor rulling out many of the physical properties such as conductivity and optical absorption. In the organic solar cells field thiophene-based polymers cyclopentadithiophene(CPDT) polymers are interesting because of their high conductivities and narrow band gaps.[9] Cyclopentadithiophene-based copolymers have shown promising power conversion efficiencies in bulk heterojunction organic photovoltaic devices of up to 3.8 %.[20]

The motivation of the present work was to contribute to first detailed study of the photophysical properties an indigo-[dodecyl-CPDT] copolymer together with the oligomeric model compound.

3.2 Results and Discussion

The structures and acronyms of the investigated compounds are depicted in Scheme 3.2, consisting of an alternating Indigo-[dodecyl-cyclopentadithiophene] copolymer together with the monomeric model compound. In addition the

spectroscopic and photophysical properties of the unsubstituted- and dodecyl-substituted cyclopentaditiophene precursors have also been investigated for comparison purposes.

R= H, CPDT
R= C$_{12}$H$_{25}$, C12CPDT

Model Compound

IND-CPDT
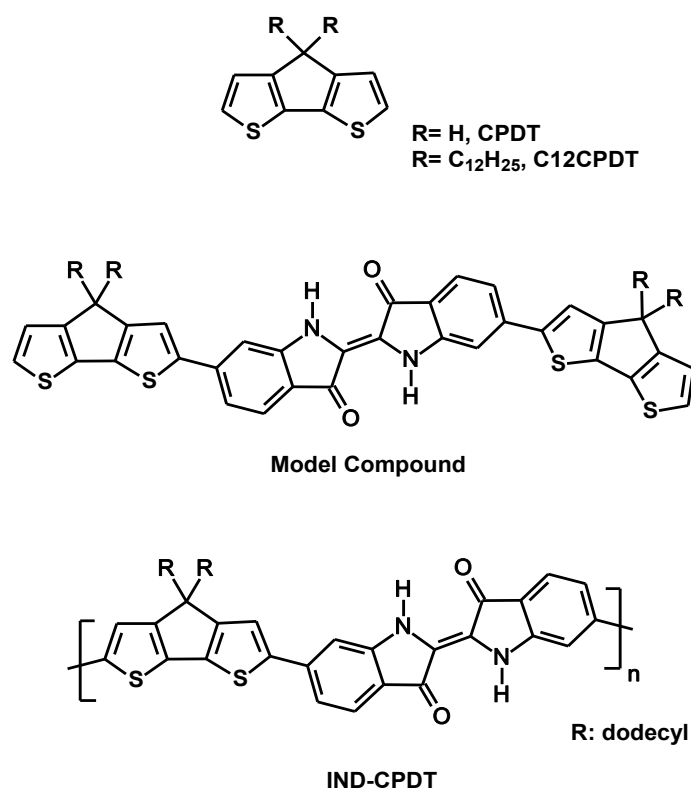
R: dodecyl

Scheme 3.2 Structures of the alternating Indigo-[dodecyl-cyclopentadithiophene] copolymer together with the monomeric model compound and the unsubstituted- and dodecyl-substituted cyclopentaditiophene precursors.

3.2.1 Singlet State

Figure 3.1 presents the absorption and fluorescence emission spectra of the CPDT and C12CPDT precursors in methylcyclohexane (MCH) solution. From the absorption and emission spectra it can be seen that the introduction of the dodecyl side chains in CPDT originates an ~8 nm redshift both in the absorption and emission spectra.
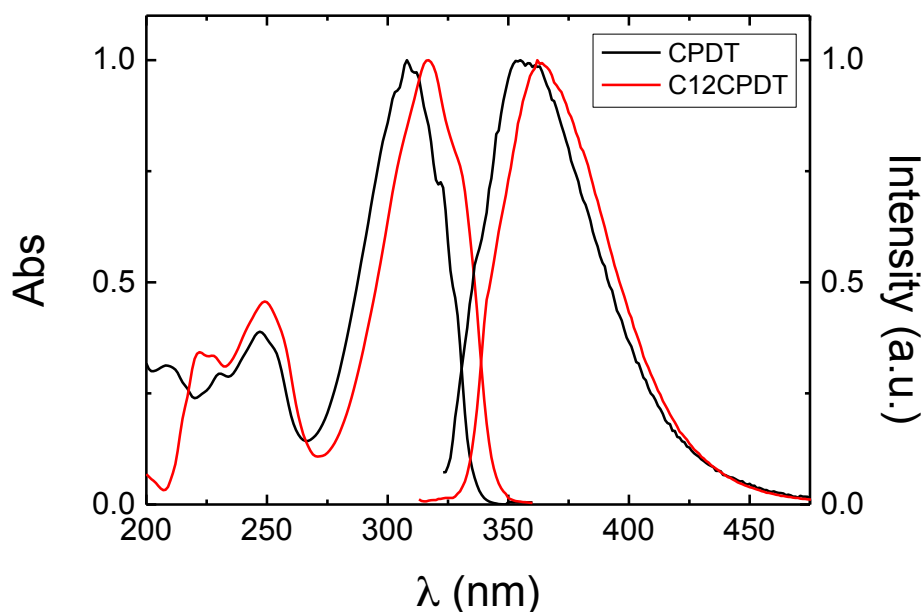
Figure 3.1 Normalized absorption and fluorescence emission spectra for CPDT and C12CPDT in methylcyclohexane solution at 293 K. Emission spectra obtained with λ_{exc}= 300 nm

The absorption spectra of the indigo-[dodecyl-cyclopentadithiophene] polymer (Ind-CPDT) and model oligomer (MC), together with those of the isolated dodecyl-cyclopentathiophene and indigo chomophoric units are presented in Figure 3.2. The absorption spectra of the oligomeric and polymeric Ind-CPDT derivative display the characteristic absorption features of the chromophoric units (although red-shifted) together with an additional "in-between" band with absorption maximum in the 517-550 nm range (see Figure 3.2 and Table 3.1). Upon going from the monomeric model compound to the copolymer a significant red shift of ~21-33 nm is observed for all the absorption spectra. In addition, for the copolymer the significant red-shift (33 nm) of the intermediary absorption band when compared to the model compound originates a high superposition with the low-energy absorption band, thus, this band appears as a shoulder of the low energy absorption band. When comparison is made between the indigo chromophore and the oligomer and copolymer under investigation, a significant red-shift of 19 nm and 41 nm, respectively, are found for the low-energy absorption. This behavior points to an extended π-conjugated character between the indigo moiety (H-chromophore) and the cyclopentadithiophene unit. It is also relevant to stress out that from the comparison of the absorption spectra of the MC (with one indigo unit) that

52

band corresponding to the indigo absorption (H-chromophore) is sharper than that displayed by In-CPDT and indigo itself. Additionally, the absorption features of the "in-between" absorption band in the investigated compounds are in agreement to what was previously observed for indigo-fluorene copolymers and thus can be assigned to a charge transfer transition.[28]
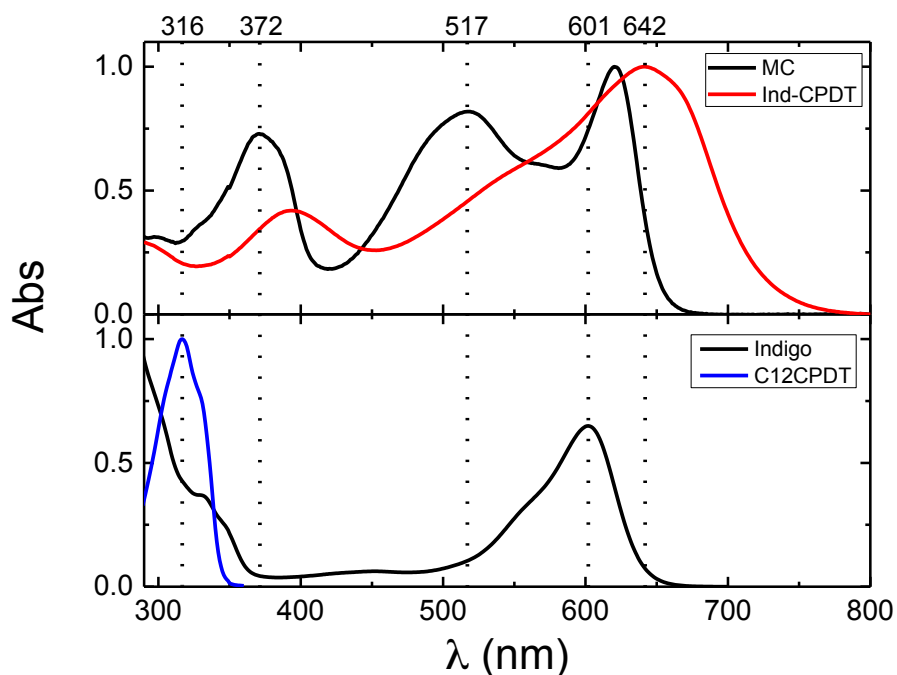
Figure 3.2 Room temperature normalized absorption spectra for the model compound (MC) and indigo-[dodecyl-cyclopentadithiophene] copolymer (Ind-CPDT) in toluene solution, together with the spectra of indigo in dioxane solution and dodecyl-cyclopentadithiophene in methylcyclohexane solution. The vertical dashed lines are guidelines to the eye.

Table 3.1 Spectroscopic (absorption, fluorescence and phosphorescence emission and triplet absorption maxima) and photophysical data (including fluorescence, ϕ_F, and phosphorescence, ϕ_{Ph}, quantum yields and lifetimes, τ_F, τ_{Ph} and τ_T) for the samples investigated in toluene solution unless stated.

Cp	λ_{max}^{Abs} (nm) 293 K	λ_{max}^{Fluo} (nm) 293 K	λ_{max}^{Phosph} (nm) 77 K	$\lambda_{max}^{T_1 \to T_n}$ (nm) 293 K	ϕ_F 293 K	τ_F (ps) 293 K	ϕ_{Ph} 77 K	τ_{Ph} (ms) 77 K	τ_T (µs) 293 K
CPDT[a]	308	355	610	370	0.01	50	0.004	5.5	26
C12CPDT[a]	316	363	610	370	0.05	50, 230	0.004	5.9	64
Indigo	285, 601	645	—	540[d]	0.0023[c]	0.14[c]	—	—	30
MC	372, 517, 620	650	—	720	0.004[b]	50	—	—	2.9
Ind-CPDT	393, 550, 642	656	—	740	0.002[b]	70	—	—	6.5

[a] Data in methylcyclohexane solution; in the case of C12CPDT two components are observed in the fluorescence decays.

[b] Data obtained with λ_{exc}= 552 nm

[c] Data in DMF taken from ref.[19].

[d] Obtained by Pulse Radiolysis in benzene solution in the presence of biphenyl or naphthalene as triplet sensitizers.[19]

Figure 3.3 presents the fluorescence emission spectra of the model compound and copolymer collected at several excitation wavelengths. A broader and red-shifted (6 nm, see Table 3.1) low-energy emission is seen for the copolymer when compared to the oligomeric unit, while no high-energy emission band is observed for the copolymer (see the spectra of the solvent in Figure 3.3 for comparison purposes with the emission signal of the copolymer at higher energies). In agreement to what was observed in the absorption spectra the spectral features of the low-energy emission shows that an extended conjugative interaction across the indigo and CPDT units should occur.

In order to explore and support the possible occurrence of intramolecular energy transfer from the CPDT moiety to the indigo unit in the copolymer the fluorescence excitation spectra was collected along the low-energy emission band, see Figure 3.4. Despite (i) the emission spectra of the investigated copolymer when excitation is performed in the CPDT related absorption band (λ_{exc}= 385 nm) displays the characteristic emission of the indigo moiety and (ii) the fluorescence excitation spectra collected in the indigo-related emission band matches the absorption characteristic absorption bands of the copolymer, it is not possible to conclude unequivocally,based only in the steady-state fluorescence study, on the occurrence of intramolecular energy transfer since in this copolymer direct excitation of the indigo is always possible (see Figure 3.2).
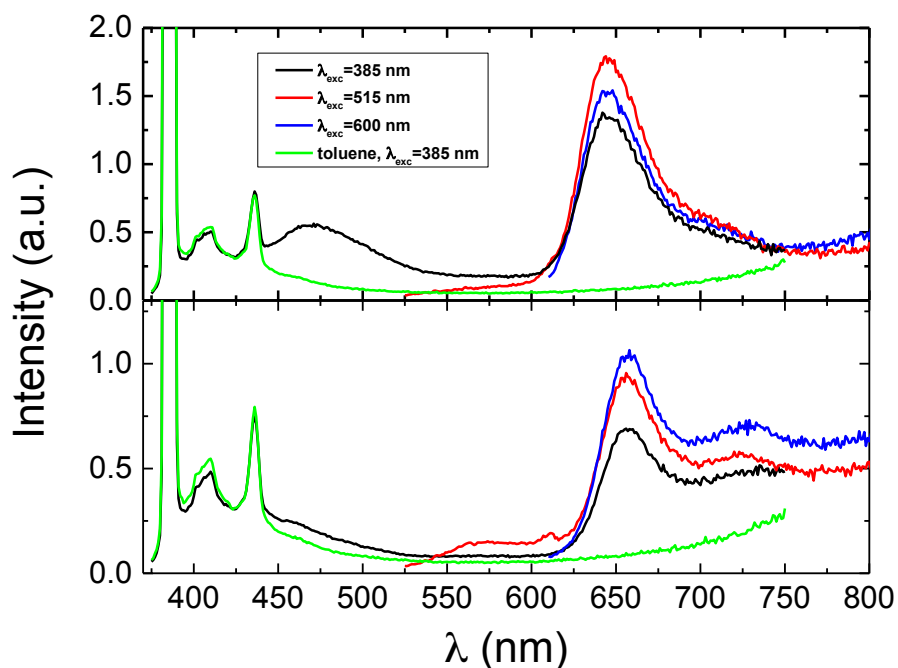
Figure 3.3 Fluorescence emission spectra for the copolymers (top panel) and model compound (bottom panel) collected at different excitation wavelengths in toluene solution at 293 K. For comparison purposes the spectra of the solvent toluene with excitation at 385 nm was also included.

The fluorescence quantum yields (ϕ_F) and correspondent lifetimes (τ_F) in methylcyclohexane and toluene solutions are presented in Table 3.1. Within experimental error, no significant changes are found in the ϕ_F values between (i) the cyclopentadithiophene derivatives (ϕ_F values in the 0.01-0.05 range); (ii) the oligomeric model compound and copolymer (values in the 0.002-0.004 range) when excited into the absorption band of the indigo moiety (λ_{exc}= 552 nm).These values are in good agreement with the fluorescence quantum yield found for indigo in dimethylformamide solution (ϕ_F= 0.0023), see Table 3.1.

Figure 3.4 Normalized absorption and fluorescence excitation spectra for the copolymer in toluene solution at 293 K.

Fluorescence lifetimes for the oligomeric model compound and copolymer were obtained with λ_{exc}= 385 nm and collected in the along the indigo-related emission band using a 3 ps time-resolution ps-TCSPC, see Figure 3.5. For both compounds, in general, the fluorescence decay times do not show any signifi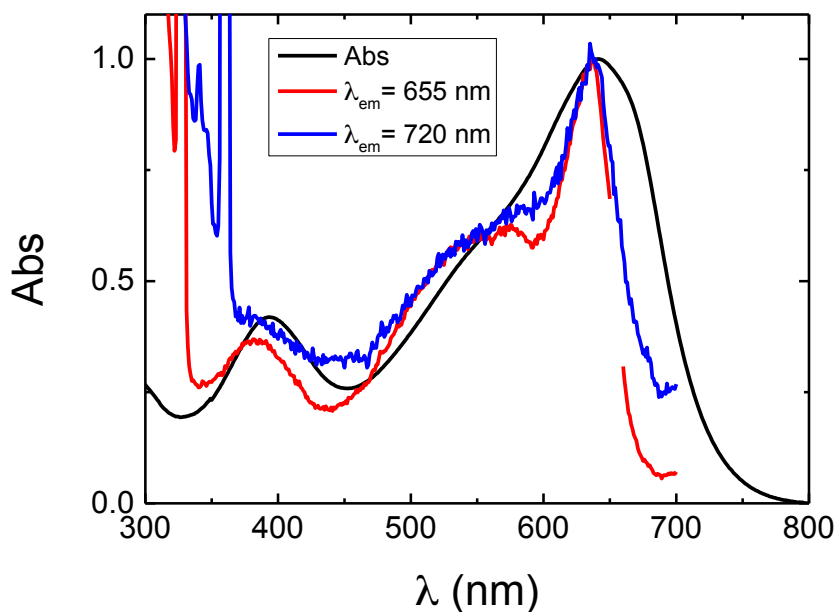cant difference when collected along the low-energy emission band and can be considered to be independent of the emission wavelength over the whole range studied. However, the same is not true for the pre-exponential factors. This calls for a global analysis of the fluorescence decays. The decay analysis of the model compound and copolymer in toluene solution reveals that these are well fitted with a sum of two exponentials: a fast decay component with 20 ps for both compounds and a longer decay time (with 50 ps for the MC and 70 ps for Ind-CPDT), see Figure 3.5. As listed in Figure 3.5, the ps-TCSPC decays collected at the shortest wavelengths (at the onset of the emission band) are dominated by the 20 ps decay which gradually loses importance (as seen by the decrease in the associated preexponential factor) with the increase in the emission wavelength, appearing as a rising component (negative preexponential value) at λ_{em}> 645 nm, MC, and λ_{em}> 660 nm, Ind-CPDT. In addition, it is possible to see, from Figure 5, that with the increase in the emission wavelength the absolute negative value of the pre-exponential value

57

associated with the short decay time increases concomitantly with the increase/dominance of the longer decay component at lower energies. This means that on the tail of the emission band the longer decay components are being formed during the decay of the 20ps component, a typical signature of the occurrence of fast relaxation processes in the excited state manifold. In previous works, these relaxation processes have been attributed either to excitation energy migration along the polymer to lower energy conjugated segments or to conformational relaxation processes in the first singlet excited state.[25,29,30] However, for the oligomeric model compound the energy transfer process should be inoperative and so the fast decay component can be attributed to torsional relaxation from an instantaneously formed excited state that rapidly relaxes to a lower energy excited state conformation. In the case of the copolymer these two processes can be operative (energy transfer and conformational relaxation) together with ESPT from the N-H to the C=O groups of indigo. In order to highlight the contribution of these processes in the excited state of the copolymer further studies are mandatory. The study of the copolymer in solvents of different viscosity and as function of temperature using ultrafast femtosecond-Transient absorption and ps-TCSPC is under progress. Because there is an activation energy barrier associated to the torsional relaxation process the associated rate constant should be temperature-dependent, whereas this dependence is absent when energy transfer is the dominant process. In addition, the study of oligomeric model compounds and in particular of their time-resolved fluorescence behavior in solvents with different viscosity is often used to obtain further information on the nature of the fast relaxation processes.[29]
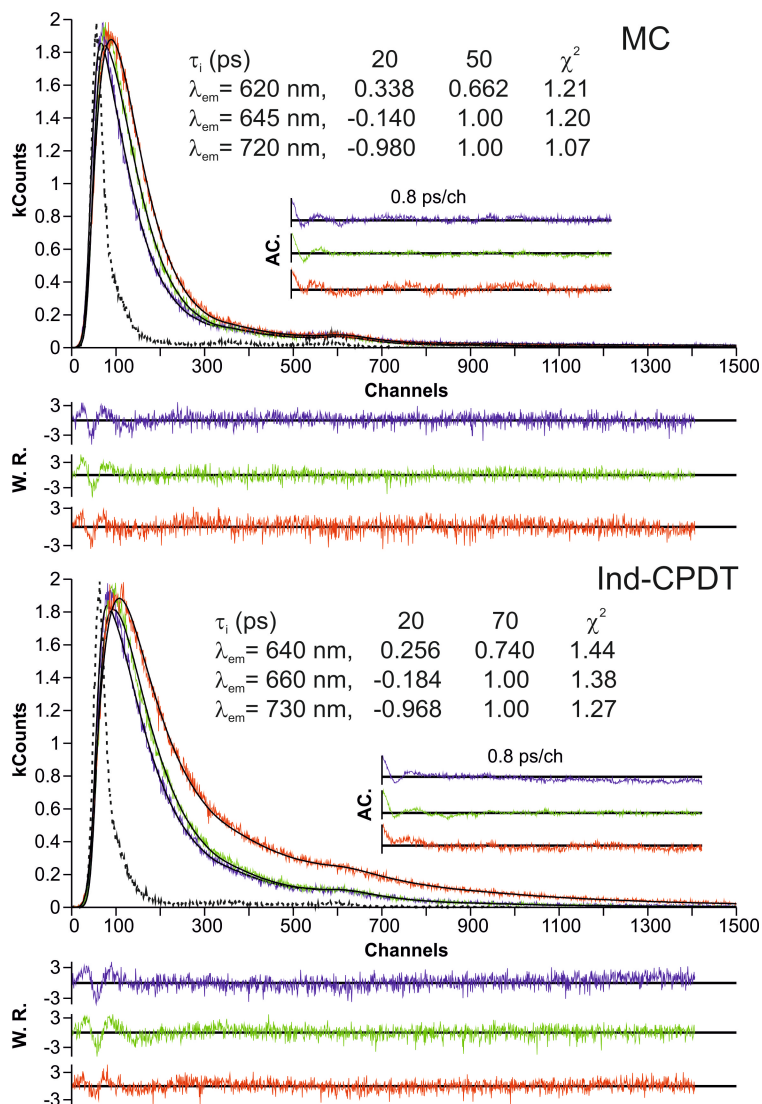
Figure 3.5 Fluorescence decays for the model compound and indigo-[dodecyl-cyclopentadithiophene] copolymer obtained with λ_{exc}= 385 nm in toluene solution at 293 K. For a better judgment of the quality of the fits, weighted residuals (W.R.), autocorrelation functions (A.C.) and χ^2 values are also presented. The dashed line in the decays is the instrumental response function.

3.2.2 Triplet State

In contrast to indigo and indigo derivatives, where no phosphorescence emission is observed, fused oligothiophene derivatives are known to show phosphorescence.[31] Indeed for the cyclopentadithiophene derivatives under investigation a broad and vibrationally structured phosphorescence emission bands were observed in frozen methylcyclohexane solution, 77 K, (Figure 3.6).

Similar phosphorescence quantum yields (ϕ_{Ph}= 0.004) and lifetimes (τ_{Ph}= 5.5-5.9 ms) were found for these derivatives, see Table 3.1. In contrast to these observations, for the model compound and copolymer no signal was observed that could be attributed to phosphorescence emission.
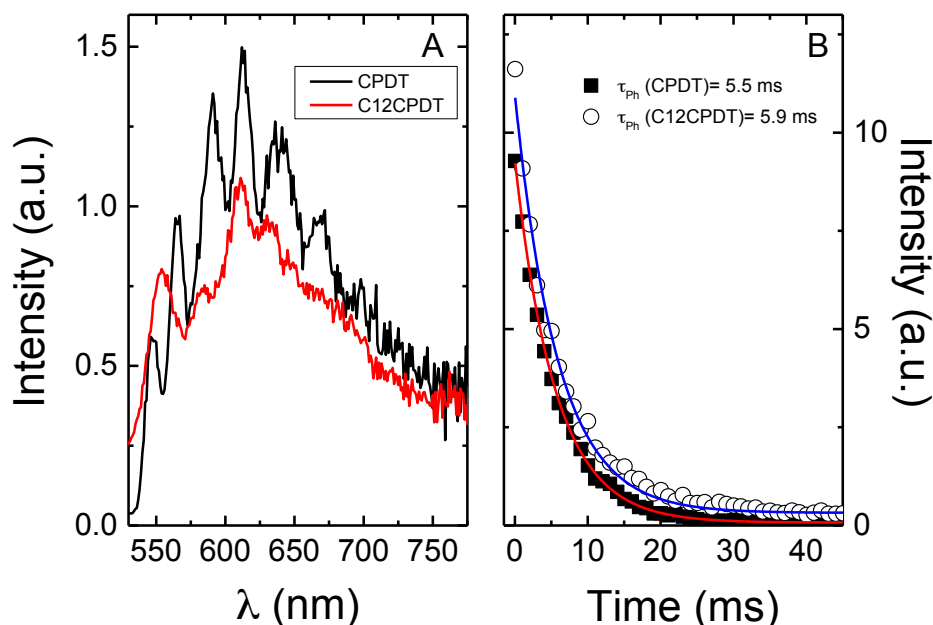
Figure 3.6 Phosphorescence emission spectra (A) and decays (B) for CPDT and C12CPDT in methylcyclohexane solution at 77 K. λ_{exc}= 355 nm

Figure 3.7 presents the transient triplet-triplet absorption spectra following laser flash photolysis at 355 nm of degassed solutions of the model compound and copolymer in comparison to the cyclopentaditiophene derivatives (excitation at 266 nm). For the cyclopentadithiophene derivatives similar triplet-triplet absorption spectra and maxima (370 nm) together with triplet lifetimes (τ_T= 26-64 μs) were found, see Figure 3.7 and Table 3.1. In the case of the oligomeric model compound and copolymer in addition to ground-state depletion at shorter wavelengths broad triplet-triplet absorption bands in the 650-800 nm region were found (Figure 3.7 and Table 3.1). The transient triplet-triplet absorption spectra and triplet lifetimes (τ_T = 2.9-6.5 μs) of the investigated oligomer and copolymer when compared with the data obtained for indigo in benzene solution (transient absorption in the 450-700 nm region and τ_T= 30 μs)[19],

shows the high degree of electronic delocalization/interactions involving the indigo and cyclopentadithiophene units in the triplet state.
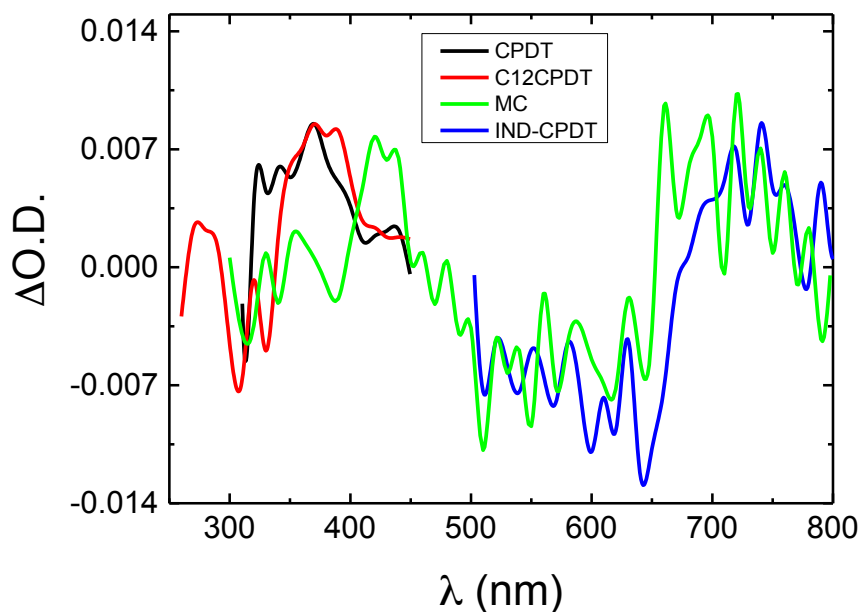
Figure 3.7 Normalized transient singlet–triplet difference absorption spectra for the cyclopentadithiophene derivatives in methylcyclohexane together with the oligomeric model compound and copolymer in toluene solution at T= 293 K.

3.3 Conclusions

The spectroscopic and photophysical properties of an alternating indigo-[dodecyl-cyclopentadithiophene] copolymer and oligomeric model compound have been evaluated in solution. It was seen that extended conjugative interaction across the indigo and CPDT units occurs in the singlet and triplet excited states. Furthermore, the occurrence of possible energy transfer and/or conformational relaxation processes in the excited state of the copolymer was equated, however, with the present data is not possible to conclude on this subject. Further studies are undergoing, namely ultrafast femtosecond-transient absorption and ps-TCSPC studies as a function of solvent viscosity and temperature.

The next step in this study is the characterization of the copolymer and oligomeric counterpart in the solid state and their photovoltaic characterization in bulk heterojunction organic solar cells.

3.4 References

1. Rondao, R.; Seixas de Melo, J.; Schaberle, F. A.; Voss, G. Physical Chemistry Chemical Physics 2012, 14, 1778.

2. L. Meijer, N. G., L. A. Skaltsounis and G. Eisenbrand, 2006, Indirubin, the red shade of indigo.

3. L. G. Wang and S. K. Mencher, i. I., the red shade of indigo, ed. L. Meijer, N. Guyard, L. A.   Skaltsounis and G. Eisenbrand 2006, Indirubin, the red shade of indigo, 247.

4. Yamazaki, S.; Sobolewski, A. L.; Domcke, W. Physical Chemistry Chemical Physics 2011, 13, 1618.

5. M. Montalti, A. C., L. Prodi and M. T. Gandolfi 2006,2008, 7, 1353.

6. G. Voss, M. D., S. Eller, M. Gradzielski, D. Gunzelmann, S. Mondal, S. van Smaalen and C. S. Voertler 2009, 92 2675.

7. Mei, J.; Graham, K. R.; Stalder, R.; Reynolds, J. R. Organic Letters 2010, 12, 660.

8. Stalder, R.; Mei, J.; Reynolds, J. R. Macromolecules 2010, 43, 8348.

9. Lambert, T. L.; Ferraris, J. P. Journal of the Chemical Society, Chemical Communications 1991, 752.

10. De Melo, J. S. S.; Rondão, R.; Burrows, H. D.; Melo, M. J.; Navaratnam, S.; Edge, R.; Voss, G. ChemPhysChem 2006, 7, 2303.

11. Schmidt, H. Chemie in unserer Zeit 1997, 31, 121.

12. Steingruber, E. In Ullmann's Encyclopedia of Industrial Chemistry; Wiley-VCH Verlag GmbH & Co. KGaA: 2000.

13. Głowacki, E. D.; Voss, G.; Sariciftci, N. S. Advanced Materials 2013, 25, 6783.

14. Qu, S.; Tian, H. Chemical Communications 2012, 48, 3039.

15. Nielsen, C. B.; Turbiez, M.; McCulloch, I. Advanced Materials 2013, 25, 1859.

16. Robb, M. J.; Ku, S. Y.; Brunetti, F. G.; Hawker, C. J. Journal of Polymer Science Part A: Polymer Chemistry 2013, 51, 1263.

17. Ho, C.-C.; Chang, S.-Y.; Huang, T.-C.; Chen, C.-A.; Liao, H.-C.; Chen, Y.-F.; Su, W.-F. Polymer Chemistry 2013, 4, 5351.

18. Guo, C.; Sun, B.; Quinn, J.; Yan, Z.; Li, Y. Journal of Materials Chemistry C 2014, 2, 4289.

19. Hong, W.; Chen, S.; Sun, B.; Arnould, M. A.; Meng, Y.; Li, Y. Chemical Science 2015, 6, 3225.

20. Lee, S. K.; Seo, J. H.; Cho, N. S.; Cho, S. Thin Solid Films 2012, 520, 5438.

21. Becker, R. S.; Seixas de Melo, J.; Maçanita, A. L.; Elisei, F. J. Phys. Chem. 1996, 100, 18683.

22. Magde, D.; Brannon, J. H.; Cremers, T. L.; Olmsted, J. The Journal of Physical Chemistry 1979, 83, 696.

23. Olmsted, J. The Journal of Physical Chemistry 1979, 83, 2581.

24. M. Montalti, A. C., L. Prodi and M. T. Gandolfi 2006.

25. Pina, J.; Seixas de Melo, J.; Burrows, H.; Maçanita, A.; Galbrecht, F.; Bunnagel, T.; Scherf, U. Macromolecules 2009, 42, 1710.

26. Stricker, G.; Subramaniam, V.; Seidel, C. A. M.; Volkmer, A. J. Phys. Chem. B 1999, 103, 8612.

27. Pina, J.; Burrows, H.; Becker, R.; Dias, F.; Maçanita, A.; Seixas de Melo, J. The Journal of Physical Chemistry B 2006, 110, 6499.

28. Pina, J.; Seixas de Melo, J. S.; Eckert, A.; Scherf, U. Journal of Materials Chemistry A 2015, 3, 6373.

29. Fron, E.; Deres, A.; Rocha, S.; Zhou, G.; Mullen, K.; De Schryver, F. C.; Sliwa, M.; Uji-i, H.; Hofkens, J.; Vosch, T. J. Phys. Chem. B 2010, 114, 1277.

30. Ferreira, B.; da Silva, P. F.; Seixas de Melo, J.; Pina, J.; Maçanita, A. J. Phys. Chem. B 2012, 116, 2347.

31. Okamoto, T.; Kudoh, K.; Wakamiya, A.; Yamaguchi, S. Chemistry – A European Journal 2007, 13, 548.

Chapter 4

Experimental section

4.1 Materials and methods

The compounds investigated(Indigo-[dodecyl-cyclopentadithiophene] copolymer together with the monomeric model compound and the unsubstituted- and dodecyl-substituted cyclopentaditiophene precursors) were provided by Prof. Ulli Scherf (Uppertal University, Germany), Prof. Manuela Raposo (Minho University, Portugal) supplied (Poly(3-hexylthiophene-2,5-diyl), P3HT, coPT and HomoPT polymers together with the monomeric oligothiophene model compounds T-TPE and Br-TPE) and (five substituted aryl-bithiophenes). The synthesis, purification and properties of the samples under study have been described elsewhere. All the solvents used were of spectroscopic or equivalent grade and were used without further treatment.

4.1.1 Solid-state thin films

Thin films from the compounds were obtained with a Desktop Precision Spin Coating System, Model P6700 series from Speedline Technologies. The solid-state thin film from the samples were obtained by deposition of a few drops of solution onto a circular sapphire substrate (10 mm diameter) followed by spin-coating (2500 rpm) in a nitrogen saturated atmosphere (2 psi). Solutions for spin-coating were prepared by adding 2 mg of the samples to 15 mg of Zeonex in 200 mL toluene or MCH solution with stirring at 40 ºC for 30 min.

4.2 Absorption

Absorption measurements were carried out on Cary 5000 UV-VIS-NIR and Shimadzu UV-2100 spectrometers. The molar extinction coefficients (ε) were obtained from the slope of the plot of the absorption with (at least) six solutions of different concentrations versus the concentration (correlation values >0.999).

4.3 Steady-state fluorescence

Fluorescence measurements were recorded with a Horiba-Jobin-Yvon Fluorolog 3-2.2 and Fluoromax 4 spectrometers. Fluorescence spectra were corrected for the wavelength response of the system. Solid-state fluorescence emission spectra where obtained with a Horiba-Jobin-Yvon integrating sphere and a Hamamatsu Quantaurus QY from.

4.3.1 Fluorescence quantum yields at room temperature

Room temperature fluorescence quantum yields (ϕ_F) were determined by comparison with standards of known quantum yield. The emission quantum yields of these reference compounds should be independent of the excitation wavelength, so the standards can be used in their full absorption range. In practice the quantum yield are determined by comparison of the integrated area under the emission spectra of optically matched solutions of the samples ($\int I(\lambda)^{cp} d\lambda$) and that of the suitable reference compound ($\int I(\lambda)^{ref} d\lambda$). The absorption and emission range of the samples (cp) and reference (ref) compound should match as much as possible. The absorbance values should be kept as lower as possible to avoid inner filter effects. In these

conditions, using the same excitation wavelength, the unknown fluorescence quantum yield (ϕ_F^{cp}) is calculated using equation 4.1

$$\phi_F^{cp} = \frac{\int I(\lambda)^{cp} d\lambda}{\int I(\lambda)^{ref} d\lambda} \cdot \frac{n_{cp}^2}{n_{ref}^2} \cdot \phi_F^{ref}$$

$$(4.1)$$

where n_x is the refractive index of the solvents in which the compounds and the reference were respectively dissolved.

In cases were the absorbance of the reference and unknown compound are not matched at the excitation wavelength an additional correction is introduced in the previous equation,

$$\phi_F^{cp} = \frac{\int I(\lambda)^{cp} d\lambda}{\int I(\lambda)^{ref} d\lambda} \cdot \frac{OD_{ref}}{OD_{cp}} \cdot \frac{n_{cp}^2}{n_{ref}^2} \cdot \phi_F^{ref}$$

$$(4.2)$$

with OD_x the optical density of the reference (ref) and compound (cp) at the excitation wavelength.

4.3.2 Fluorescence quantum yields at low temperature (77 K)

The fluorescence quantum yields at 77 K were obtained by comparison with the spectrum at 293 K run under the same experimental conditions. The following equation is then applied,

$$\phi_F^{77K} = \frac{\int I(\lambda)^{77K} d\lambda}{\int I(\lambda)^{293K} d\lambda} \cdot \phi_F^{293K} \cdot f_c$$

$$(4.3)$$

66

where $\int I(\lambda)^x d\lambda$ is the integrated area under the emission of the sample at 77 K and 293 K, ϕ_F^{293K} is the fluorescence quantum yield at 293 K and f_c is the factor that considers the "shrinkage" of the solvent (volume) upon cooling, given by V77K/V293K (for ethanol and methylcyclohexane is assumed $f_c = 0.8$).

4.3.3 Solid-state fluorescence quantum yields

The solid-state fluorescence quantum yields in thin films were obtained using the integrating sphere, using the method outlined by de Mello et. al. and developed by Palsson and Monkman.The following

equation was used to determine the solid state fluorescence quantum yields (ϕ_F^{Solid}),

$$\phi_F^{Solid} = \frac{\int^{cp} I(\lambda)d\lambda}{\left(\int^{SA} I(\lambda)d\lambda - \int^{SS} I(\lambda)d\lambda\right) \cdot 10^{\Delta OD(\lambda_{exc})}}$$

(4.4)

where $\int^{cp} I(\lambda)d\lambda$ is the integrated area under the emission of the sample compound in the thin film (which excludes the integration of Rayleigh peak), $\int^{SA} I(\lambda)d\lambda$ is the integrated area under the Rayleigh peak of a sample containing only the sapphire support and $\int^{SS} I(\lambda)d\lambda$ is the integrated area under the Rayleigh peak in the emission spectra of the compounds under investigation in thin films. Since the emission from the samples is much weaker than the scattered excitation light (Rayleigh peak) the spectra is recorded with a filter that attenuates the emission intensity at the excitation wavelength. This is considered in Equation 4.4 with $10^{\Delta OD(\lambda_{exc})}$, the filter transmittance at the excitation wavelength.

4.4 Time-resolved fluorescence

The fluorescence decays were measured using a home-built picosecond TCSPC apparatus. The excitation source consists of a picosecond Spectra Physics mode-lock Tsunami® Laser (Ti:Sapphire) Model 3950 (repetition rate of about 82 MHz, tuning range 700-1000 nm), pumped by a Millennia® Pro-10s, frequency-doubled continuos wave (CW), diode-pumped, solid-state laser (lem= 532 nm). A harmonic generator model GWU-23PS (Spectra Physics) is used to produce the second and third harmonic from the Ti:Sapphire laser exciting beam frequency output. The samples where measured with excitation at 395 nm and the horizontally polarized output beam from the GWU (second harmonic) was first passed through a ThorLabs depolarizer (WDPOL-A) and after by a Glan-Thompson polarizer (Newport 10GT04) with vertical polarization. Emission at 90º geometry collected at magic angle polarization was detected through a Oriel CornerstoneTM 260 monochromator by a Hamamatsu microchannel plate photomultiplier (R3809U-50). Signal acquisition and data processing was performed employing a Becker & Hickl SPC-630 TCSPC module. The full width at half maximum (FWHW) of the IRF was about 22 ps and was highly reproducible with identical system parameters. Deconvolution of the fluorescence decays curves was performed using the Globals WE software package and the method of modulating functions of Striker.

4.5 Phosphorescence

Phosphorescence measurements were made in glasses at 77 K and used the Horiba-Jobin-Yvon Fluorolog 3-2.2 spectrometer equipped with a 1934 D phosphorimeter unit and a 150 W pulsed xenon lamp. The phosphorescence spectra were corrected for the wavelenght response of the system.

4.5.1 Phosphorescence quantum yields

The phosphorescence emission spectra from optically matched solutions (at the excitation wavelength) of the samples and the reference compound were collected and Equation 6.6 was used to determine the phosphorescence quantum yield (fPh);

$$\phi_F^{cp} = \frac{\int I(\lambda)^{cp} \, d\lambda}{\int I(\lambda)^{ref} \, d\lambda} \cdot \phi_{Ph}^{ref}$$

(4.6)

where $\int I(\lambda)^x \, d\lambda$ is the integrated area under the phosphorescence emission of the samples and the reference and ϕ_{Ph}^{ref} is the phosphorescence quantum yield of the reference compound. The phosphorescence quantum yields were determined using benzophenone (fPh= 0.84) as standard.

4.6 Room temperature singlet-oxygen phosphorescence

Room-temperature singlet oxygen phosphorescence was detected at 1270 nm with a Hamamatsu R5509-42 photomultiplier cooled to 193 K in a liquid nitrogen chamber (Products for Research model PC176TSCE-005) following laser excitation of aerated solutions at 266 nm, 355 nm or 532 nm in an adapted Applied Photophysics flash kinetic spectrometer. The modification of the spectrometer involved the interposition of a 600-line diffraction grating instead of the standard spectrometer, to extend spectral response to the infrared. the use of a Schott RG1000 filter was essential to eliminate from the infrared signal all of the first harmonic contribution of the sensitizer emission in the region below 850 nm.

4.6.1 Singlet-oxygen formation quantum yields

The singlet oxygen formation quantum yields ($\phi\Delta$) were obtained by direct measurement of the phosphorescence at 1270 nm following irradiation of aerated

solutions of the compounds. The $\phi\Delta$ values were determined by plotting the initial emission intensity for optically matched solutions as a function of the laser energy and comparing the slope with that obtained upon sensitization with the reference compound. 1H-phenalen-1-one in toluene (λexc= 355 nm, $\phi\Delta$= 0.93) or rose bengal in methanol (λexc = 532 nm, $\phi\Delta$= 0.76) were used as the standard.

$$\phi\Delta = (\text{Slope}^{\text{sample}}/\text{Slope}^{\text{STD}})*(\text{abs}_{\lambda\text{exc sample}}/\text{abs}_{\lambda\text{exc STD}})*\phi\Delta_{\text{solvent}}$$

4.7 Triplet-triplet transient absorption spectra

The experimental setup used to obtain triplet spectra and triplet lifetimes consists of an Applied Photophysics laser flash photolysis apparatus pumped by the fourth harmonic (266 nm), third harmonic (355 nm) or second harmonic (532 nm) of a Nd:YAG laser (Spectra Physics). The detection system (Hamamatsu R928 photomultipliers) is at right angle to the excitation beam, and a pulsed 150 W Xe lamp is used to analyze the transient absorption. The signal obtained is fed into a Tektronix TDS 3052B digital analyzer and transferred to an IBM RISC computer where the optical density (OD) at different wavelengths and different delays after flash are collected using the appropriate software (Applied photophysics). Transient spectra were collected by monitoring the optical density change at intervals of 5-10 nm over the range 250-850 nm and averaging at least 10 decays at each wavelength. First order kinetics were observed for the decays of the lowest triplet state. Special care was taken in order to have low laser energy ($\leq$2 mJ) to avoid multiphoton and triplet-triplet annihilation effects. Before experiments were taken, all solutions were degassed with nitrogen for $\approx$20 min and sealed.